

# Indonesian Journal of Science & Technology





# Cost, Emission, and Thermo-Physical Determination of Heterogeneous Biodiesel from Palm Kernel Shell Oil: Optimization of Tropical Egg Shell Catalyst

Samuel O. Effiom<sup>1</sup>, Fidelis I. Abam<sup>2</sup>, Precious O. Effiom<sup>2</sup>, Thomas O. Magu<sup>3</sup>, Emmanuel E. John<sup>1</sup>, Olusegun D. Samuel<sup>4,5\*</sup>, Burhan Saeed<sup>6</sup>, Macmanus C. Ndukwu<sup>7</sup>, Christopher C. Enweremadu<sup>5</sup>, Muhammad Latifur Rochman<sup>8</sup>, Muji Setiyo<sup>8,\*</sup>

<sup>1</sup>Cross River University of Technology, Calabar, Nigeria

<sup>2</sup>University of Calabar, Calabar, Nigeria.

<sup>3</sup>University of Chinese Academy of Science, Beijing, China

<sup>4</sup>Federal University of Petroleum Resources, Effurun, Delta State, Nigeria

<sup>5</sup>University of South Africa, Florida, South Africa;

<sup>6</sup>University of Portsmouth, England, United Kingdom

<sup>7</sup>Michael Okpara University of Agriculture Umudike, Umudike, Nigeria

<sup>8</sup>Universitas Muhammadiyah Magelang, Magelang, Indonesia

\*Correspondence: E-mail: samuel.david@fupre.edu.ng, muji@unimma.ac.id

#### **ABSTRACTS**

The advantages of reusability, lower cost, and environmentally friendly operation have made the heterogeneous catalyzed methylic process a preferable alternative to the homogeneously catalyzed protocol. The optimal production yield of palm kernel shell oil (PKSO) methyl ester (PKSOME) was modeled using Response Surface Methodology (RSM). The cost of PKSOME was determined, and the synthesized PKSOME was blended with diesel fuel with various volume ratios. Several analyses were done, including thermophysical properties using ASTM test methods, density and viscosity, fire point and flash point, aniline point, and acid value. Emission characteristics such as exhaust smoke, carbon monoxide, and carbon dioxide were measured using an IC engine. The use of waste eggshells for heterogeneously catalyzed biodiesel from underutilized PKSO for green diesel can reduce production costs even further. The green biodiesel model and TP correlations have applications in the biodiesel and aviation industries.

© 2024 Tim Pengembang Jurnal UPI

# ARTICLE INFO

#### Article History:

Submitted/Received 15 Aug 2023 First Revised 11 Sep 2023 Accepted 08 Nov 2023 First Available online 09 Nov 2023 Publication Date 01 Apr 2024

#### Keyword:

Biodiesel, Emission, Heterogeneous catalyst, Optimization, Response surface methodology, Thermophysical properties.

#### 1. INTRODUCTION

The increased use of fossil fuels for transportation and energy has resulted in ozone layer destruction and health risks for people worldwide (Gururani et al., 2022; Fattah et al., 2013). As a result of the current global energy crisis, traditional fossil fuels have been replaced by alternative or renewable sources (Ampah et al., 2022; (Setiyo et al.; 2021; Nayaggy & Putra, 2019; Maheshvari, 2022). Alternate energy sources are currently being researched to reduce environmental carbon footprints and increase energy efficiency (Adekoya et al., 2022). As part of this research center's alternative energy resource, biodegradable materials are used as feedstock in the conversion processes to produce biofuel or hydrogen or pyrolytic oils that can replace fossil fuels (Atelge, 2022; Kolakoti et al.; 2022; Pebrianti & Salamah, 2021). Biofuels are generated through a variety of processes, including physiochemical (transesterification, esterification), thermochemical (pyrolysis, gasification), and biochemical (anaerobic digestion, fermentation) (Osman et al., 2021; Bhikuning & Senda, 2020).

Transesterification is a chemical reaction resulting in biodiesel production (BPR), which can be used for transportation and power generation (Dwivedi et al., 2022). When biodiesel is used as an additive to conventional fossil diesel, emissions of particulates, carbon monoxide, and hydrocarbons are reduced (Nema et al., 2023). It is possible to use it in its purest form. The absence of aromatic and sulfur compounds contributes to biodiesel's compatibility with diesel engines (Veza et al., 2022). However, biodiesel made from food-grade vegetable oils is too expensive to compete on a cost basis with fossil-based diesel, as it would reduce the global food bank (Bardhan et al., 2015). Non-edible vegetable oil/plant oil is preferred as a feedstock for BPR because it is an agricultural waste product (Singh et al., 2020). Because of ethical and financial concerns, inedible oils such as jatropha, castor, and rubber seed oils have been used to produce biodiesel in developing countries. Sub-Saharan Africa has an abundance of major feedstocks for BPR.

In developing countries, inedible oils such as jatropha, castor, rubber seed oils, and palm kernel oil have been used to produce biodiesel because of ethical and cost concerns (Kareem et al., 2022). Countries in Sub-Saharan Africa have an abundance of major feedstocks for BPR (Moser, 2009). Among the feedstocks, palm kernel shell (PKS) from these palm oil mills is underutilized and a nuisance to the community (Oti et al., 2017). The waste generated by the global palm oil industry contains more than 70% PKS, making disposal difficult (Abdul Malek et al., 2020; Rupani et al., 2022). This waste must be disposed of properly. However, palm kernel oil can be extracted from shells and used to make biodiesel (Abdul Aziz et al., 2017). This suggests that green diesel is the most effective way to keep the PKS from becoming a nuisance. Rupani et al. (2022) attributed the palm kernel shell oil (PKSO)'s suitability to fuel properties and prominent lauric feature compared to average ligr Brown icollip recessitates alcohol and a catalyst in the transesterification process. To accelerate the reaction, either homogeneous (HOCs) or heterogeneous catalysts (HECs) can be used. Because of the benefits of HECs over HOCs, such as ease of separation, dual production process, high efficiency and reusability, functional surface, the economy of production, lower corrosion, low cost, and safe environmentally friendly operation (Qu et al., 2021). Tang et al. (2018) and Amesho et al. (2022) indicated that using biowaste-derived HEC from agricultural wastes could reduce environmental pollution while also allowing for easy separation of biodiesel from glycerol. Renewable sources such as eggshells (Faroog et al., 2018), seashells (Mazaheri et al., 2018), tucuma shells (Mendonça et al., 2019), bamboo ash (Liu et al., 2018), cocoa pods (Ofori-Boateng & Lee, 2013), palm kernel (Bazargan et al., 2015), coconut shell (Thushari et al., 2019), and red banana peduncle (Balajii & Niju, 2019),

Sugarcane bagasse biochar (Hidayat et al., 2021) have been used to develop catalysts for BPR. For the HEC, eggshell has been chosen over other renewable resources because of their affordability, favorable impact on biodiesel yield and viscosity, ease of reusing, and long-term viability (Faroog et al., 2018; Kirubakaran, 2018). Transesterification parameters like reaction time, molar ratio, and catalyst dosage have been found to impact biodiesel yield. Increasing yield and lowering production costs can be accomplished by optimising these variables (Samuel et al., 2022a; Haryanto & Telaumbanua, 2020). The use of Response Surface Methodology (RSM) to forecast and model the transesterification process has been highly promoted because of its simplicity and ability to correlate input variables with responses (Samuel et al., 2022b). HEC biodiesel production from third-generation feedstock oils has been predicted and modeled using the RSM technique (Ghosh & Halder, 2022; Singh et al., 2018). Table 1 summarizes the adoption of the RSM approach adopted to boost BPR from oily feedstocks by several researchers (Adepoju et al., 2018; Ajala et al., 2022; Balajii & Niju, 2019; Betiku & Ajala, 2014; Dhawane et al., 2015; Ishola et al., 2019; Kumar et al., 2021; Narula et al., 2017; Qu et al., 2021; Sarve et al., 2015; Singh et al., 2020). As noted, the RSM has not been used to evaluate the dosage of eggshells as an HEC in enhancing green diesel production from PKSO.

**Table 1.** A concise overview of the optimization of biodiesel types from assorted oils.

	Catalyst		Transes	Yield (%)	Refs.		
Feedstock	type	Catalyst dosage	M/O	Time	Tem (°C)		
Palm oil	Zn-Ce/Al2O3	8.19	18.53	-	66.12	99.44	Qu <i>et al</i> . (2021)
Ceiba pentandra oil	<i>Musa</i> acuminata peduncle	2.68	11.46	106 min	-	98.73	Balaji and Niju (2019)
Waste lard	CaO-Al <sub>2</sub> O <sub>3</sub> - SiO <sub>2</sub> -CaSO <sub>4</sub> -	5.0	12.0	1hr	59.97	96.35	Ajala <i>et al</i> . (2022)
Preutilized cooking oil	Eggshell- coconut pith	5.0%	8:1	60 min	-	72	Kumar <i>et al</i> . (2021)
Microalgal oil	β-strontium silicate	2.5	12:1	104 min	65	97.88	Singh <i>et al</i> . (2020)
Sorrel oil	-	1.23	8:1	43 min	65	99.71	Ishola <i>et al</i> . (2019)
Lucky nut oilseed	Pearl spar	2.5	2.5:1	50 min	-	92.8	Adepoju <i>et al</i> . (2018)
algal oil	CaO and CaO/Al <sub>2</sub> O <sub>3</sub>	1.56	3.2:10 v/v	125	50	88.89	Narula <i>et al</i> . (2017)
Sesame oil	Barium hydroxide	1.79	6.69:1	40.30 min	31.92	98.6	Sarve <i>et al</i> . (2015)
Hevea brasiliensis oil	Flamboyant pods derived steam activated carbon	3.5	15:1	-	-	89.3	Dhawane et al. (2015)
Neem oil	Cocoa pod husk	0.65	0.73 v/v	-	65oC	99.3	Betiku and Ajala (2014)

The environmental friendliness of biodiesel adoption in diesel engines is dependent on its lower pollutant emissions. Running diesel engines on fossil diesel results in increased nitrogen oxide emissions, rising fossil diesel prices, and a significant decline in its reserve. Researchers recently switched HEC biodiesel to power diesel to avoid the abovementioned challenges. To assess the environment-friendliness of green diesel, emission features such as carbon dioxide, carbon monoxide, and exhaust smoke are investigated (Singh et al., 2020). The emission characteristics of IC engines running on HEC biodiesels are highlighted in **Table 2**. So far as we know, the environmental friendliness of HEC-based PKSO biodiesel exhaust from IC engines has not been studied.

A review of previous studies demonstrated that the RSM could predict HEC based-biodiesel from various second-generation oily feedstocks and its diverse engine characteristics in IC engines. Furthermore, the RSM model demonstrates its capability in enhancing HEC-based biodiesels from various oils and establishing its capacity to detect the appropriate dosage of the catalyst to accelerate the rate of the methylic process. As a result of the RSM model's extraordinary development in efficiency and correlation of multi-input parameters and response chosen for optimization and modeling of BPR in the study.

**Table 2.** An overview of engine characteristics of IC engines fuelled with heterogeneous biodiesel.

Types of heterogeneous (HE) biodiesel	Types of catalyst	Types of diesel engine	Emission features of IC engine	Refs.
HEC-WCO biodiesel	TiO₂ nano- catalyst	DI	UHC, CO, and NOx, BTE,	Elkelawy <i>et al</i> . (2022)
HEC-WCO biodiesel	zinc doped calcium oxide	NS	CO, HYC, NO <sub>x</sub> , smoke opacity	Kataria <i>et al</i> . (2019)
HEC used oil biodiesel	ram bone	4S, WC, VCR, DI	CO and hydrocarbon (HYC) emissions engine exhaust temperature (EET) and fuel consumption (FC)	Pradhan <i>et al</i> . (2018)
HEC-waste mustard oil biodiesel	Amberlyst 15	NS	CO, HYC	Pradhan <i>et al</i> . (2016)
HEC-algae biodiesel	K <sub>2</sub> CO <sub>3</sub> /ZnO	IS, WC, 4 stroke, DI	BTE, CO, HYC	Nair <i>et al</i> . (2020)
HEC-karanja biodiesel	Li-CaO	IS, WC, 4 stroke, DI	BTE, BSFC, exhaust gas temperature, smoke opacity, NO <sub>x</sub> , CO, CO <sub>2</sub>	Patel <i>et al</i> . (2020)
HEC-chicken fat biodiesel	Eggshell		CO, NOx, HYC, smoke	Kirubakaran (2018)
HEC-Pongamia oil biodiesel	KI/CaO	NS	CO, UBCH, smoke opacity, NO <sub>x</sub>	Anjana <i>et al</i> . (2016)

As a result of using only one variable at a time, the palm kernel industry's implementation of a viable and reliable tool for modeling oil waste from its mills has been twisted. However, the studies are notable for (1) modeling of the transesterification variables for low FFA PKSO with fewer experimental runs at a lower cost and (2) a reliable and straightforward tool for enhancing and engaging in biorefinery of dual operating of oil processing and converting the oil from the palm kernel shell to green diesel, as well as powering diesel engines and heating elements.

BPR from many 2nd generation oil feedstocks is well documented in the literature. Still, HEC-based biodiesel from PKSO and the use of eggshells which are underutilized and discarded from local chicken poultry in Nigeria as a heterogeneous catalyst are yet to be implemented. To further reduce costs and make green diesel more environmentally friendly, it is essential to adapt and prepare domestic discard such as eggshells that are currently underutilized for HECs in the future.

The use of PKSO as a promising source of biodiesel synthesis is innovative in this study. Despite a decade of research on heterogeneous catalyzed biodiesel using second-generation oil (SGO) and waste-based catalyst (WBC), to the author's knowledge, the use of PKSO as the SGO and eggshell as the WBC has not been documented. Additionally, the emission characteristics of an IC engine fuelled by eggshell-catalyzed PKSO biodiesel have not been published. The prior study's purpose was to look into the RSM's applicability for optimizing and modeling PKSO methyl ester (PKSOME) production and establish regression equations for key thermophysical parameters of its PKSO methyl esters with fossil diesel blends. The study also looks at the viability of biodiesel made from PKSO and its effectiveness in diesel engines by assessing the environmental friendliness of cleaner fuel. The use of cleaner fuel will pave the way for the conversion of dual waste to wealth, and the preservation of the environment's ecosystem.

#### 2. METHODS

## 2.1. Material, Catalyst Preparation, and Its Characterization

In this research, eggshells from local fowl from tropical poultry in Nigeria were adopted for the development of HEC. Moreover, methanol and pretreated PKSO were accosted for the transesterification process. The thermophysical properties of PKSO are presented in **Table 3**.

Deionized water was used to wash the eggshells and dried them in an oven overnight. The shell as a heterogeneous catalyst is prepared and modified following the methods described elsewhere (Yaşar, 2019; Zhao et al., 2018). To speed up the methylation process of PKSO, the material was modified and calcined. The flask was heated to reflux for two hours with 100 ml of concentrated phosphoric acid added to the eggshell. During reflux, the outer jacket of the reflux condenser's reflux condenser was allowed to circulate water. The steam in the flask was not lost due to this action. After the mixture had been cooled, the solids were removed using high-quality filter paper (240 mm). After drying in a hot air oven at 60°C, the residue was transferred to ceramic crucibles and calcined for four hours at 600°C in a muffle furnace to convert CaCO<sub>3</sub> to CaO.

The catalyst was also subjected to FTIR and SEM analyses to identify its functional groups and determine its surface morphology and internal microstructure (Nandiyanto et al., 2023). This will help determine whether this catalyst is suitable for BPR. The molecular vibrations of catalysts were revealed by the FTIR at wavelengths ranging from 500 to 4000 cm<sup>-1</sup>. The morphologies of the catalyst were observed using SEM images. The results were also compared with several mathematical equations, in which the nomenclature is presented in **Table 3**.

Table 3. Nomenclature.

Symbol	Information					
A, B, C, D; E, F, G; H, I, J; K,	regression constants in the respective fuel					
L, M; N, O, P; Q, R, S						
AP	aniline point					
$A_s$	Agitation speed					
$A_s^2$	Quadratic of agitation speed					
AV	Acid value					
$C_d$	Catalyst dosage					
$C_d$ ME: PKSO	Interaction of catalyst amount and molar ratio					
$C_d^2$	Quadratic of catalyst dosage					
$C_d^{^{^{\prime\prime}}}$	Product of catalyst dosage and reaction temperature					
$C_d A_s$	Product of catalyst dosage and agitation speed					
$C_d R_{te}$	Product of catalyst dosage and reaction temperature					
$C_d R_t$	Product of catalyst dosage and reaction time					
$C_d A_s$	Product of catalyst dosage and agitation speed					
ME: PKSO	Methanol/ palm kernel seed oil molar ratio					
ME: PKSO <sup>2</sup>	Quadratic of methanol/ palm kernel seed oil molar ratio					
ME: PKSOR <sub>te</sub>	Interaction of molar ratio and reaction temperature					
ME: PKSOR <sub>t</sub>	Interaction of molar ratio and reaction temperature					
ME: PKSO	Interaction of methanol and palm kernel shell oil					
ME: PKSO <sup>2</sup>	Quadratic of Intera of methanol and palm kernel shell oil					
R <sub>te</sub>	Reaction time					
$R_{te}^{2}$	Quadratic of reaction time					
$R_t^{i\epsilon}$	Reaction temperature					
$R_t^{^{^{\prime}2}}$	Quadratic of reaction time					
$R_{te}R_{t}$	Interaction of reaction temperature and time					
$R_{te}A_{s}$	number of data					
$R_t A_s$	regression coefficient					
RSM	Response Surface Methodology					
Y <sub>PKSOME</sub>	Yield of palm kernel seed oil methyl ester					
Greek	,					
$\nu$	kinematic viscosity					
$\in_1$ , $\in_{ii}$ , $\in_{ij}$	interaction coefficients					
Xi and Xj	independent variables					
$\epsilon_1$	Constant					

# 2.2. Extraction of PKSO from Shell, Production of PKSO Methyl Esters, and Defemination of Fuel Properties with Diesel Fuel Blends

The palm kernel oil extraction is as follows: The palm kernel shell was obtained from local mill residue dump sites. To remove impurities, the product was air-dried and sorted. It was then ground further in an industrial blender. The sample was placed in the thimble of a 500 ml Soxhlet extractor after being weighed into a semi-permeable cotton material. After that, the n-hexane was measured in a 500 ml flask with a flat and round bottom. The condenser connected to the round flask with n-hexane and Soxhlet with extraction thimble containing the sample in the semi-permeable membrane. The Soxhlet extraction system was heated on a hot plate while water circulated through the condenser's outer jacket. When all the oil had been extracted, the process was terminated. Distill the oil-n-hexane mixture contained in the flat bottom flask after stripping the defatted sample from the semi-permeable membrane. The extracted oil was kept in the flask while the n-hexane was distilled.

24.3

895

33.20

The process specifications for the methanolysis process for PKSO from pre-treated PKSO are as follows: The high FFA of PKSO was reduced using the esterification reaction variables (1.0 wt.% of catalyst amount ( $H_2SO_4$ ) concentration, 60 min reaction duration, and 6:1 methanol/oil molar) were detected to pre-treat high fatty acid PKSO to permit base methanolysis (see **Table 4**).

Density	Viscosity	Acid number	Saponification	Pour	Flash point
(kg/m³)	(@ 40 °C (mm <sup>2</sup> s <sup>-1</sup> )	(mg KOH/g)	value (mg KOH/g)	point (°C)	(°C)

239.7

Table 4. Physicochemical properties of PKSO (Samuel & Emovon, 2018).

Costa et al. (2022) and Kim et al. (2020), PKSO having high fatty acid (12.4 mg KOH/g oil) was esterified to render base methanolysis operative. Figure 1 portrays the procedure specifications for producing biodiesel from pre-treated esterified PKSO. Mixing potassium hydroxide and methanol resulted in the potassium methoxide mixture. Potassium methoxide was added to hot-esterified PKSO in a lab-scale reactor. The PKSOME was allowed to settle after the transesterification operation was completed. Eqs. (1) was used to estimate the PKSOME yield in the experiments performed:

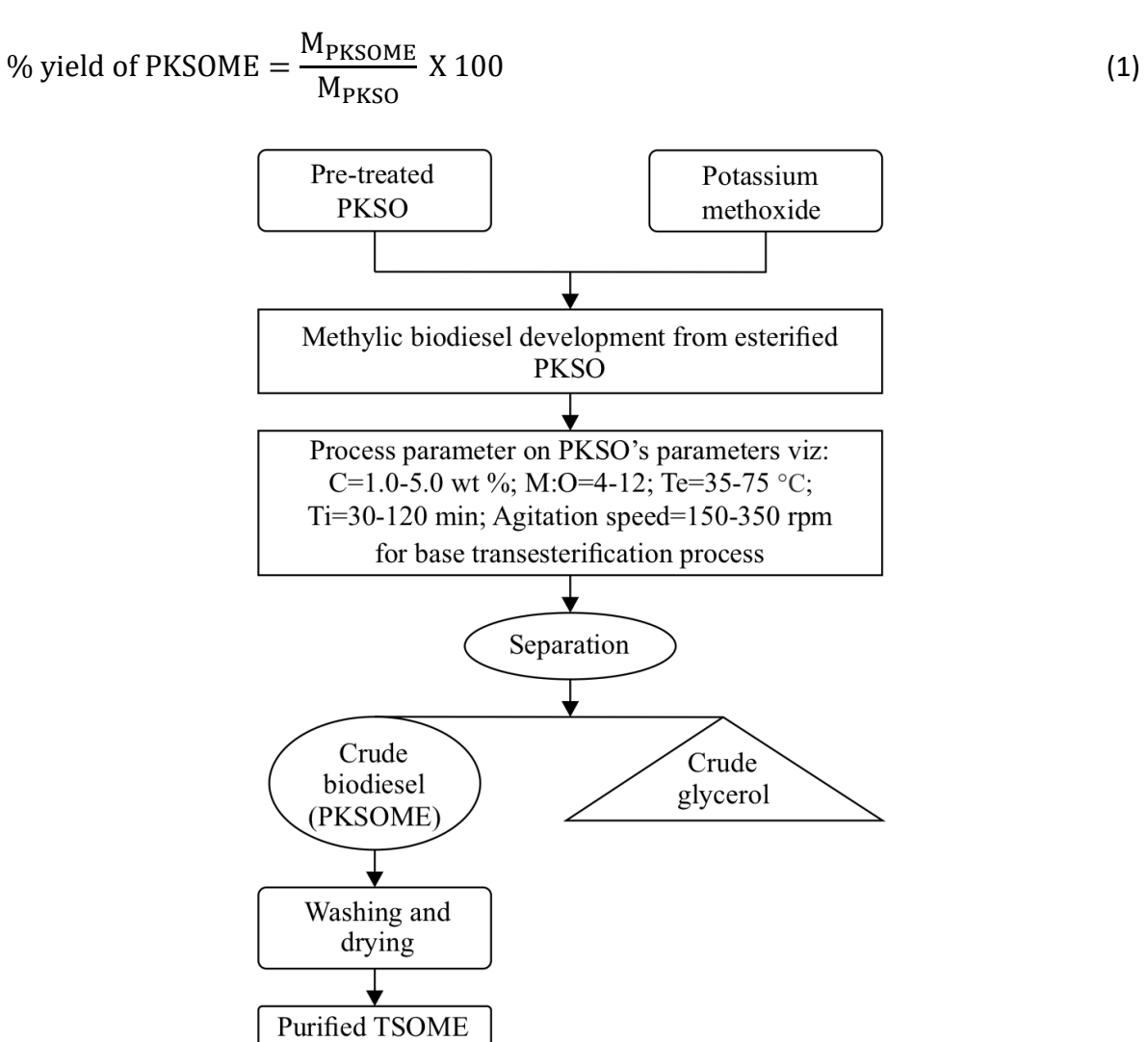


**Figure 1.** Production of PKSOME.

242

20

#### 2.3. Cost Analysis

For determining the cost of BPR from PKSO. As can be seen, the cost includes the expenses related to the BPR from 1 liter of PKSO, methanol, KOH, labor, electricity, catalyst preparation, and miscellaneous. **Figure 2** shows the schematic for the mathematical computation of the BPR from PKSO, while **Figure 3** demonstrates the cost comparison of the component of BPR from PKSO.

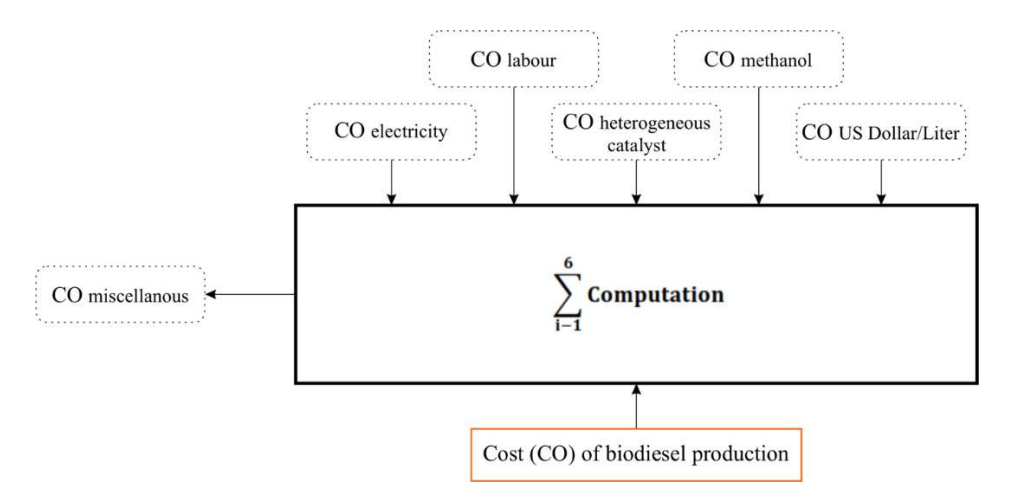


Figure 2. Schematic for the cost of BPR.

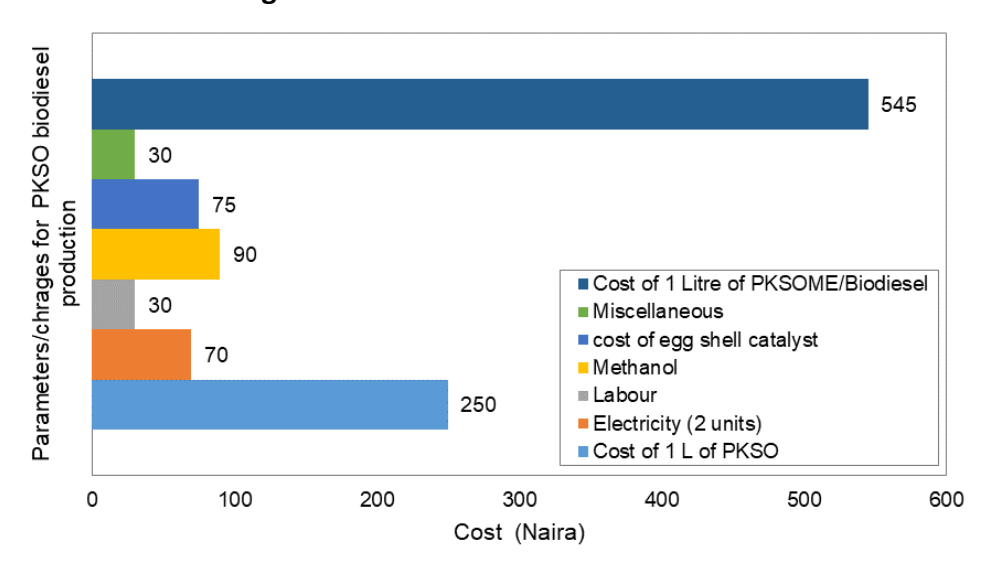


Figure 3. Cost assessment for BPR from PKSO.

# 2.4. Models for Approximating the Basic Thermophysical Properties of PKSOME-Diesel Fuel Blends

The fuel types were B0 (diesel fuel), B10 (10%), B20 (20%), B30 (30%), B40 (40%), and B100 (100%). **Table 5** provides a summary of the equipment and procedures used to evaluate thermophysical properties. The density and kinematic viscosity of the fuel types are detected to be correlated using polynomial and quadratic expressions using **Eqs. (2)** and **(3)**, respectively. The fire point (FIP), flash point (FP), aniline point (AP), and acid value (AV) of the fuel types are detected to be correlated with biodiesel content using **Eqs. (4)**, **(5)**, **(6)**, and **(7)**, respectively.

9 | Indonesian Journal of Science & Technology, Volume 9 Issue 1, April 2024 Hal 1-32

$$D_{PKSOME} = Ax^3 - Bx^2 + Cx + D \tag{2}$$

$$KV_{PKSOME} = -Ex^2 + Fx + G (3)$$

$$FIP_{PKSOME} = Hx^2 + xI + J \tag{4}$$

$$FP_{PKSOME} = Kx^2 + Lx + M (5)$$

$$AP_{PKSOME} = Nx^2 + Ox + P (6)$$

$$AV_{PKSOME} = Qx^2 + Rx + S (7)$$

**Table 5.** Accuracy of equipment employed for the fuel property measurements.

Property	Standard method	Equipment	Accuracy
Density, 15 °C	ASTM D1250	Density hygrometer	-
Kinematic viscosity, 40 °C	ASTM D445	Chongqing viscometer	$0.5 \text{ mm}^2/\text{s}$
Flash point	ASTM D56	Pensky-Martens flash tester	0.1 °C
Fire point	ASTM D5901	Pensky Martens apparatus	0.1 °C
Acid value	ASTM D664	Automated titration system	$\pm$ 0.001 mgKOH/g
Aniline Point	ASTM D611-12	Aniline point apparatus	±0.1 °C
Diesel index	ASTM D611	Aniline point apparatus	±0.1 °C
Cetane number	ASTM D4737	Cetane analyser	NS

NS=not specified

# 2.5. Modeling of PKSOME Production using the RSM Approach

The RSM model in Design-Expert software was utilized in this study to assess the impact of varying the reaction time, the methanol/oil molar ratio, and the dosage of catalysts used on the yield of HEC PKSOME. As shown in **Figure 4**, the RSM model is used to create biodiesel from PKSO. The ranges of transesterification variables (TVs) such as catalyst dosage ( $C_d$ ) and methanol/PKSO molar ratio (ME: PKSO), reaction temperature ( $R_{te}$ ), reaction time ( $R_t$ ), and agitation speed (As) are chosen as discussed elsewhere (Samuel *et al.*, 2020a; 2022b) and selected.

The measured ranges for the used TVs were respectively 1.0-5.0 wt%, 4.0-12.0, 35-75 °C 30-120 min, and 150-350 rpm. The rotatable central composite design (RCCD) merged with the RSM was used to obtain 32 experimental terms without needless iterations. This was used to further investigate the five aforementioned factors' impact on PKSOME production (See **Table 6**). The superiority of the quadratic equation response model was checked by the significance test and analysis of variance (ANOVA). The fitted model is represented in **Eq. (8)**.

$$Y_{PKSOME} = \in_0 + \sum_{i=1}^k \in_1 x_i + \sum_{i=i}^k \in_{ii} x^2_i + \sum_{i=1}^{k-1} \sum_{j=1}^k \in_{ij} x_i x_j + \varepsilon$$
 (8)

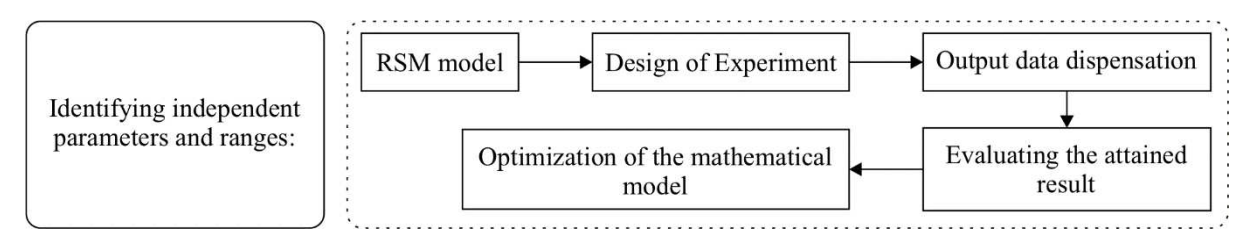


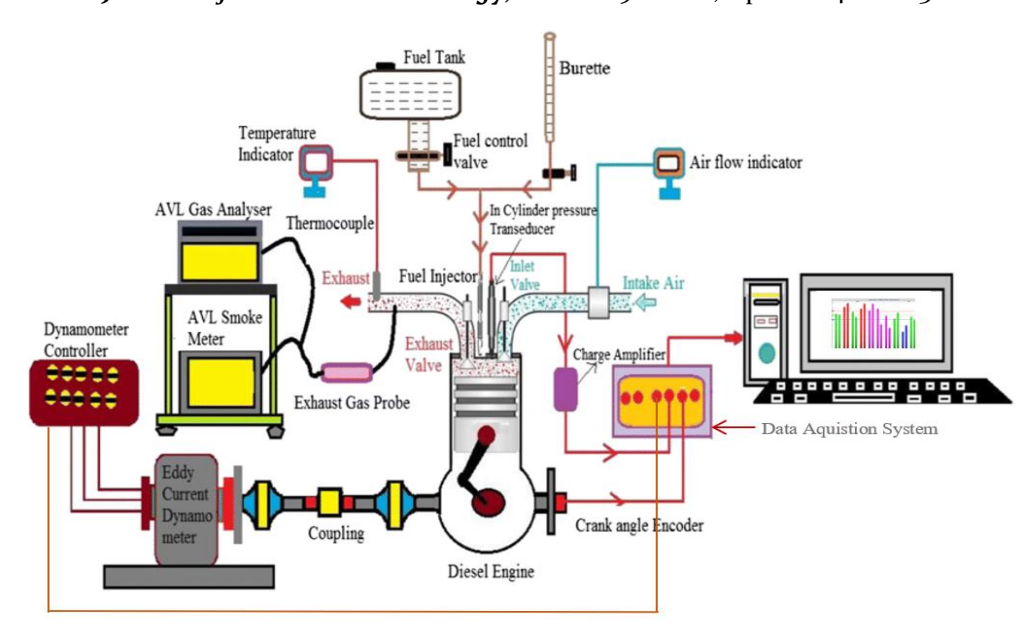
Figure 4. Flow chart for RSM model.

Table 6. Experimental design layout.

	Response									
Run order	Catalyst dosage (wt %)	Methanol/Oil molar ratio	Reaction temperature (°C)	Reaction time (Minutes)	Agitation seed (rpm)	Biodiese yield (%)				
1	4	4	45	90	150	46.83				
2	1	12	75	150	200	68.40				
3	3	12	65	90	350	72.98				
4	4	4	55	30	350	44.72				
5	1	4	35	30	150	35.65				
6	1	12	35	30	350	39.66				
7	1	12	45	90	150	49.41				
8	3	12	65	30	250	43.83				
9	5	12	35	30	150	39.04				
10	1	8	75	60	350	58.97				
11	3	8	35	60	250	49.17				
12	5	8	55	90	250	64.11				
13	1	4	45	90	300	45.28				
14	4	12	35	90	350	53.67				
15	5	8	55	90	250	68.43				
16	5	8	55	90	250	68.43				
17	1	6	35	150	150	46.29				
18	2	8	55	150	350	65.70				
19	4	12	45	150	200	57.24				
20	5	6	75	120	350	71.58				
21	3	12	65	30	250	40.16				
22	5	12	75	150	350	76.05				
23	4	10	75	120	150	67.44				
24	5	4	75	30	200	39.39				
25	3	4	75	150	250	63.80				
26	1	12	35	150	250	43.18				
27	1	6	65	30	150	34.22				
28	5	4	35	150	350	39.70				
29	5	10	65	30	150	37.85				
30	2	8	55	150	350	69.30				
31	3	8	35	60	250	45.76				
32	4	4	45	90	150	50.48				

# 2.6. Emission Quality Assessments

In this study, to investigate the environmental friendliness of biodiesel, the gas analyzer was adopted to detect the exhaust emission quality tests of the PKSOME. A diesel engine (single cylinder with model Lombardini DIESEL 3LD 510) portrayed in **Figure 5** with full specification in **Table 7** was adopted. For the measurement of pollutant emissions, a gas analyzer was placed on the line of engine exhaust gases. Emissions of exhaust smoke, carbon monoxide, and carbon dioxide are measured using an exhaust gas analyzer, and smoke meter.



**Figure 5.** Schematic setup of diesel test bed.

Table 7. Engine specification.

Parameter	Specification
Engine type	Single-cylinder, four-stroke, water-cooled, compression ignition (CI) engine
Bore	82 mm
Stroke	110 mm
Compression ratio	16.5:1
Speed	1500 rpm
Rated Power	3.7 Kw
Cubic capacity	556.24 cc

# 2.7. Uncertainty Evaluation of Diesel/PKSOME Fuelled IC Engine

There are numerous operational and physical test engine parameters, resulting in some uncertainty. As a result, an uncertainty analysis in terms of experimentation precision coupled with repeatability is imperative for safeguarding the accuracy of the experimental setup (Singh *et al.*, 2019). The uncertainty of all measurements is abridged in **Table 8**. As can be realized, the estimation of crucial important parameters is provided. The measuring equipment's uncertainty analysis was carried out using the standard method specified elsewhere. The experiment's overall uncertainty analysis was determined using **Eq. (9)**.

**Table 8.** Uncertainty assessment of Perkins test engine.

Inst	rument	Accuracy		
Load indicator		±0.01 kW	±0.15	
Temperature indicator		±1 °C	±0.05	
Burette		±0.2 cm <sup>3</sup>	±0.2	
Pressure transducer		±0.1bar	±0.05	
Speed sensor		±10 rpm	±0.1	
Crank angle encoder		±1°	±0.2	
Exhaust gas analyzer	(Exhaust smoke)	0.02%	±0.2	
	$(CO_2)$	0.05%	±0.2	
	(CO)	0.06%	±0.2	

#### 3. RESULTS AND DISCUSSION

### 3.1. Features of the Catalyst

According to Nandiyanto *et al.* (2019), Obinna, 2022, and Nandiyanto *et al.* (2023), the functional groups were identified using FTIR analysis. **Figure 6** depicts the FTIR analysis results for the functional groups found in the egg shell catalyst. As observed, O-H (acid) bonds are associated with the strongest absorbance, shown by the largest peak at 3011.7 to 2855.1 cm-1.C-O was also detected between 1000 and 1300 cm-1 and C=O between 1647.5 and 1744.4 cm-1 in the fingerprint region (See **Table 9**). The results align with previous findings published in other sources (Wongjaikham *et al.*, 2021; Sukamto & Rahmat, 2023). **Figure 7** further depicts the catalyst's morphology, particle size, and internal microstructure. The majority of the particles detected were in the nanometer range and had high porosity, indicating a high specific surface area of the catalyst (Yolanda & Nandiyanto, 2022).

Overall urcertainly = square root of 
$$((exhaust\ smoke)^2 + (CO_2)^2 + (CO)^2)$$
  
= square root of  $((0.2)^2 + (0.2)^2 + (0.2)^2)$  (9)

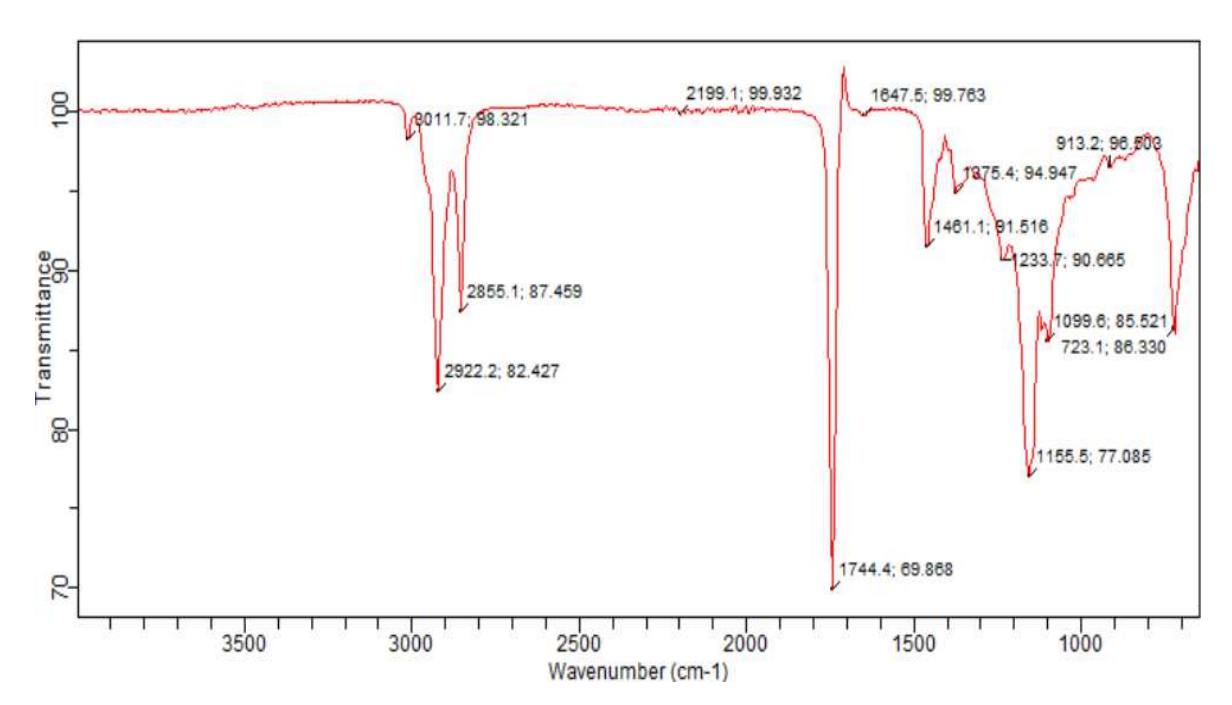


Figure 6. FTIR spectra of the egg shell catalyst.

Table 9. FTIR for PKSOME.

Wavelength	Transmittance	Functional group
3011.7	98.321	Bonded OH group
2922.2	82.427	Bonds of CH groups
2858.1	87.4959	CH stretch of alkene
2199.1	99.932	Hydrogen group stretching
1744.4	69.868	C = O stretch of esters carboxyl
1647.5	99.763	C=C stretch of linear alkene
1461.1	91.510	C-H bonds
1375.4	94.947	CH3
1233.7	90.665	C-O stretch of fatty acids methyl esters
1155.5	77.085	C-O-C stretch of esters
1099.6	85.521	C-O, esters, ethers and C-O-O
913.2	96.503	C-O-O-C stretch of peroxide
723.1	80.330	C - N bonds

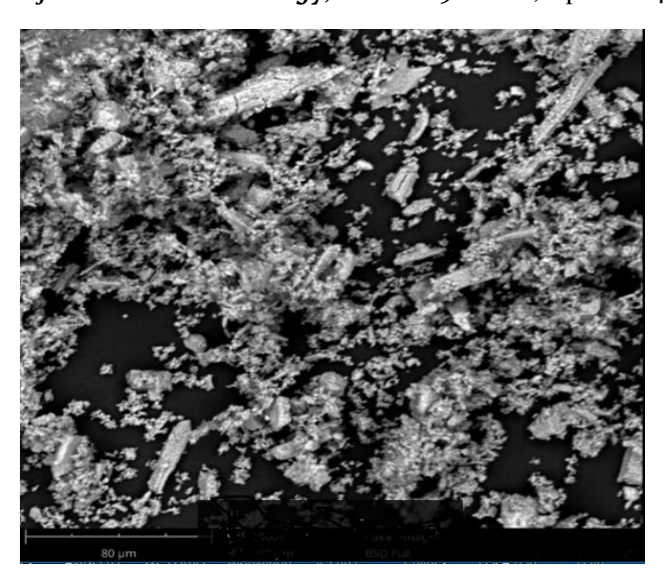


Figure 7. SEM micrograph of the egg shell catalyst.

#### 3.2. Optimization of Production of PKSOME

## 3.2.1. Analysis of variance (ANOVA)

RSM was adopted for the transesterification parameters of PKSO to predict the suitable condition. Then, the most satisfactory representations were chosen for the authentic laboratory data (ALD). The polynomial model arrogates the ALD more than the others due to the P values (<0.0001). On the other hand, the F-values of the models might be an additional measure for selecting the suitable model. The value of the models was noticed as 1225.36. Also, adjusted and predicted regression coefficients were assessed by way of 0.9987 and 0.9968, which are greater than the others. Hence, the desire for the model to suit the information.

**Table 10** summarizes the ANOVA's impacts. This examination (0.005) was sustained for significant worth or unimportance. The appraised F-value of 1225.36 with a fairly small probability value of 0.0001 was observed to be substantial at a 95% assurance level. This signifies the strength of the tailored model for predicting the production of the PKSOME. The values of  $\rm R^2$ , adjusted  $\rm R^2$ , and predicted  $\rm R^2$  were appraised to be 0.9996, 0.9987, and 0.9968, respectively. As perceived from **Table 10**, Apart from PKSO-Methanol/oil. $\rm R_{te}$ ,  $\rm C_d^2$  and  $\rm A_s^2$   $\rm C_d$  that are not significant, all other single, interactive, and squared variables are detected to be significant and influence the yield of PKSOME production. The  $\rm 2^{nd}$ -degree equation established from the dependent model in terms of real factors is specified in **Eq. (10)**.

According to **Eq. (10)**,  $Y_{PKSOME}$  is the PKSOME'yield (%),  $C_d$ , ME: PKSO,  $R_{te}$ ,  $R_t$ , and  $A_s$ , are independent variables with a single effect.  $C_d$ . ME: PKSO,  $C_d$ .  $R_{te}$ ,  $C_dR_t$ ,  $C_dR_s$ , ME: PKSO $R_{te}$ , ME: PKSO $R_s$ ,  $R_{te}R_t$ ,  $R_{te}A_s$ ,  $R_tR_{te}$  are interaction terms between the variables, whereas  $C_d^2$ , ME: PKSO $R_s$ ,  $R_{te}^2$ , and  $R_t^2$ , and  $R_t^2$  are the squared terms. The positive sign in front of the terms indicates a synergistic effect, while the negative sign indicates an antagonistic effect of the variables.

```
\begin{array}{l} Y_{PKSOME} + 62.84 + 2.62C_d + 2.73\text{ME: PKSO} + 6.17R_{te} + 9.06R_t + 3.31A_s \\ - 0.2103C_d.\,\text{ME: PKSO} - 0.7587C_d.R_{te} - 1.10C_dR_t + 0.3955C_dA_s \\ - 0.0498\text{ME: PKSO}R_{te} + 1.37\text{ME: PKSO}A_s + 2.45\text{MEPKSO}.A_s \\ + 6.34R_{te}R_t + 2.34R_{te}A_s - 1.94R_tR_{te} + 0.2307C_d^2 \\ - 5.65\text{ME: PKSO}^2 - 4.84R_{te}^2 - 6.03R_t^2 + 0.0564A_s^2 \end{array} \tag{10}
```

Source	Sum of Squares	df	Mean Square	F-value	p-value	Remarks
Model	5013.1	20	250.68	1225.36	< 0.0001	significant
$\mathcal{C}_d$ -Catalyst dosage	105.59	1	105.59	516.16	< 0.0001	significant
ME: PKSO-Methanol/oil	130.57	1	130.57	638.28	< 0.0001	significant
R <sub>te</sub> -Temperature	589.92	1	589.92	2883.66	< 0.0001	significant
R <sub>t</sub> -Reaction time	1265.2	1	1265.22	6184.71	< 0.0001	significant
$ m A_s$ -Agitation speed	172.80	1	172.80	844.70	< 0.0001	significant
$C_d$ ME: PKSO	0.3709	1	0.3709	1.81	0.2052	significant
$C_d$ R <sub>te</sub>	5.54	1	5.54	27.06	0.0003	significant
$C_d R_t$	9.43	1	9.43	46.08	< 0.0001	significant
$C_d$ A <sub>s</sub>	1.37	1	1.37	6.69	0.0253	significant
ME: PKSOR <sub>te</sub>	0.0240	1	0.0240	0.1175	0.7382	not significant
ME: PKSOR <sub>t</sub>	21.01	1	21.01	102.71	< 0.0001	significant
ME: PKSOA <sub>s</sub>	54.92	1	54.92	268.44	< 0.0001	significant
$R_{te}R_{t}$	382.82	1	382.82	1871.30	< 0.0001	significant
$R_{te}A_{s}$	55.72	1	55.72	272.38	< 0.0001	significant
$R_tA_s$	30.79	1	30.79	150.51	< 0.0001	significant
$C_d^2$	0.2359	1	0.2359	1.15	0.3059	not significant
ME: PKSO <sup>2</sup>	159.38	1	159.38	779.09	< 0.0001	significant
$R_{te}^{2}$	99.90	1	99.90	488.33	< 0.0001	significant
$R_t^{\frac{1}{2}}$	161.91	1	161.91	791.44	< 0.0001	significant
$A_s^2$	0.0179	1	0.0179	0.0877	0.7727	not significant
Residual	2.25	11	0.2046			-
Lack of Fit	0.2503	5	0.0501	0.1502	0.9724	not significant
Pure Error	2.00	6	0.3333			-
Cor Total	5015.76	31				

# 3.3. Effect of Methanolysis Variables on PKSOME's Yield

Figure 8 presents 3D response surfaces for the yield of PKSOME due to various methylic variables. Figure 8a depicts the yield of PKSOME vs. catalyst amount and reaction temperature. As observed, the yield increased with the time and catalyst dosage. The yield started to decline when the reaction time was 65 min and the catalyst dosage was 3.0 wt.%. Similar reports were also highlighted by Ong et al. (2014) and Tamilarasan & Sahadevan (2014). Rodrigues et al. (2009) and Ginting et al. (2012) attributed the reduction in the PKSOME's yield to the formation of emulsion and gel development. Figure 8b portrays the interaction between catalyst dosage and reaction time on PKSOME's yield. As observed, the yield increases with the increase in reaction time from 30 to 150 minutes and the catalyst dosage from 1 to 3wt %, respectively. Even though reaction time had a positive effect on PKSOME yield, catalyst dosage had a greater effect than reaction time (Ashine et al., 2023). Figure 8c shows the disproportion of the yield of PKSOME vs. catalyst loading and agitation speed. As seen, the yield increases with the increase in agitation speed from 150 to 300 minutes, and catalyst concentration from 1 to 3wt % respectively. A similar report was expressed by Chimezie et al. (2023). However, the yield decreased at a higher agitation speed. Figure 8d represents the interaction between the molar ratio and reaction time on PKSOME's yield. As observed, increasing reaction time and methanol/oil molar enhanced the yield. Samuel et al. (2022a) attributed the reduction in the yield at the higher molar ratio and reaction time to interfering with PKSOME parting with glycerol and hydrolysis. Figure 8f depicts the yield of PKSOME as a function of reaction time and temperature. The yield increased with the

increase in reaction time of 30 to 150 minutes and temperature of 35 to 75 °C respectively. It further indicated that the yield improved when the rapid reaction occurred at a higher reaction time and temperature. A similar result was observed by Sundaramahalingam *et al.* (2021). However, at higher temperatures above the optimal value of 65 °C, a noticeable decrease in biodiesel yield was observed. The reversible nature of the reaction and solvent vaporization, as noted by Sundaramahalingam *et al.* (2021) and Rezania *et al.* (2021), caused the yield to decrease after the optimal temperature.

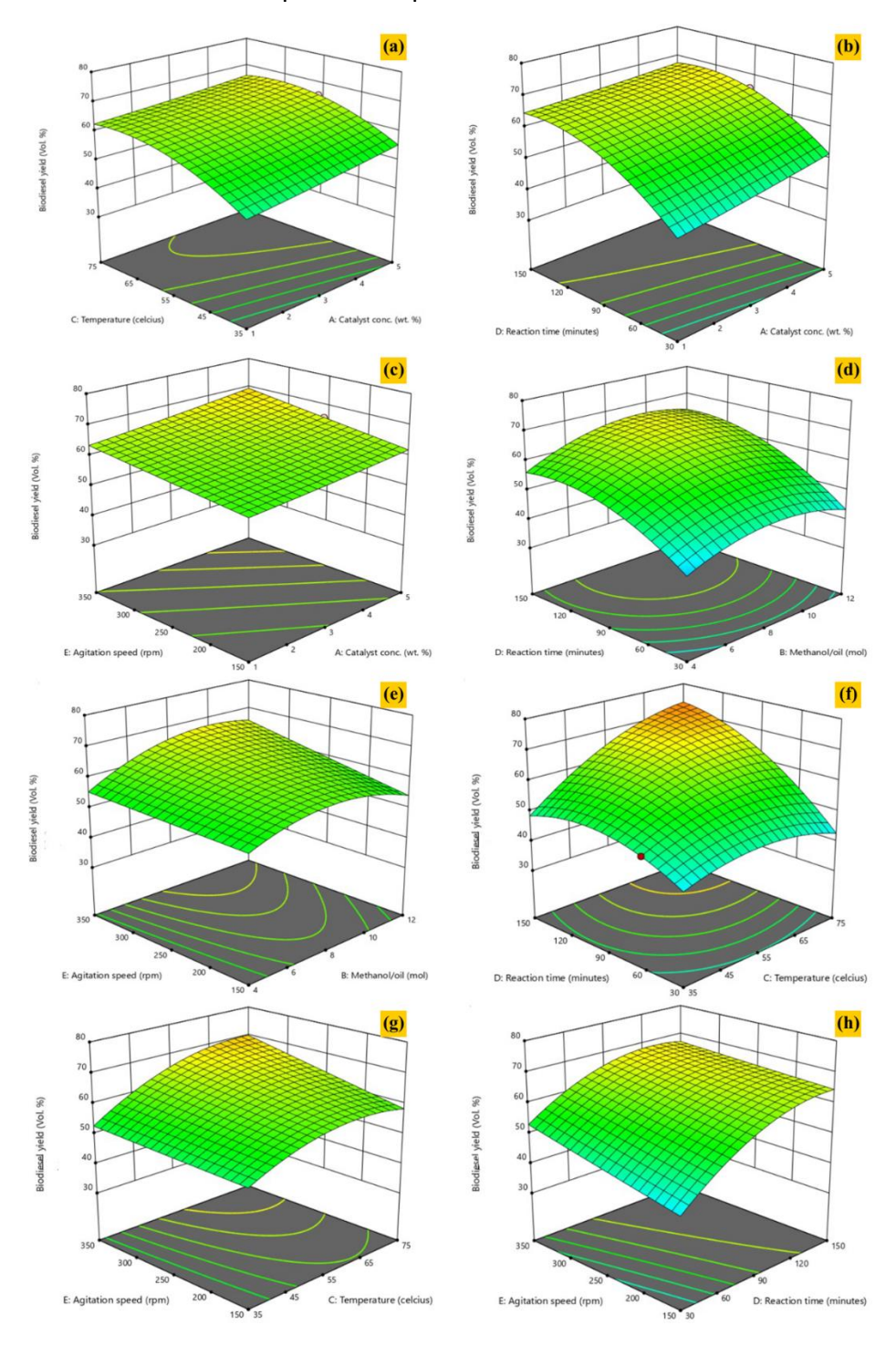


**Figure 8**. 3D plots of (a) catalyst dosage and temperature, (b) catalyst dosage and reaction time, (c) catalyst dosage and agitation speed, (d) molar ratio and reaction time, (e) molar ratio and agitation speed, (f) reaction temperature and time, (g) reaction temperature and agitation speed, and (h) reaction time and agitation speed on PSOME's yield.

Figure 8g portrays the influence of reaction temperature and agitation speed (AS) on the yield of PKSOME. The yield increased with the increase in the AS from 150 to 300 rpm and temperature of 35 to 65 °C. The enhanced yield was attributed to the rapid reaction at higher AS and temperature (Razzag et al., 2020). However, beyond the temperature range of 55-65 °C, a reduction in the yield was observed. Also, Figure 8h shows the yield of PKSOME vs. reaction time and AS. As depicted, the yield improved as reaction time and AS increased. However, at a higher AS above the optimal value, the yield of biodiesel decreased.

Figure 9 portrays the plot of actual vs. predicted PKSOME yield. As shown, the general data point aligns close to the diagonal line and displays good agreement of actual and predicted vield.

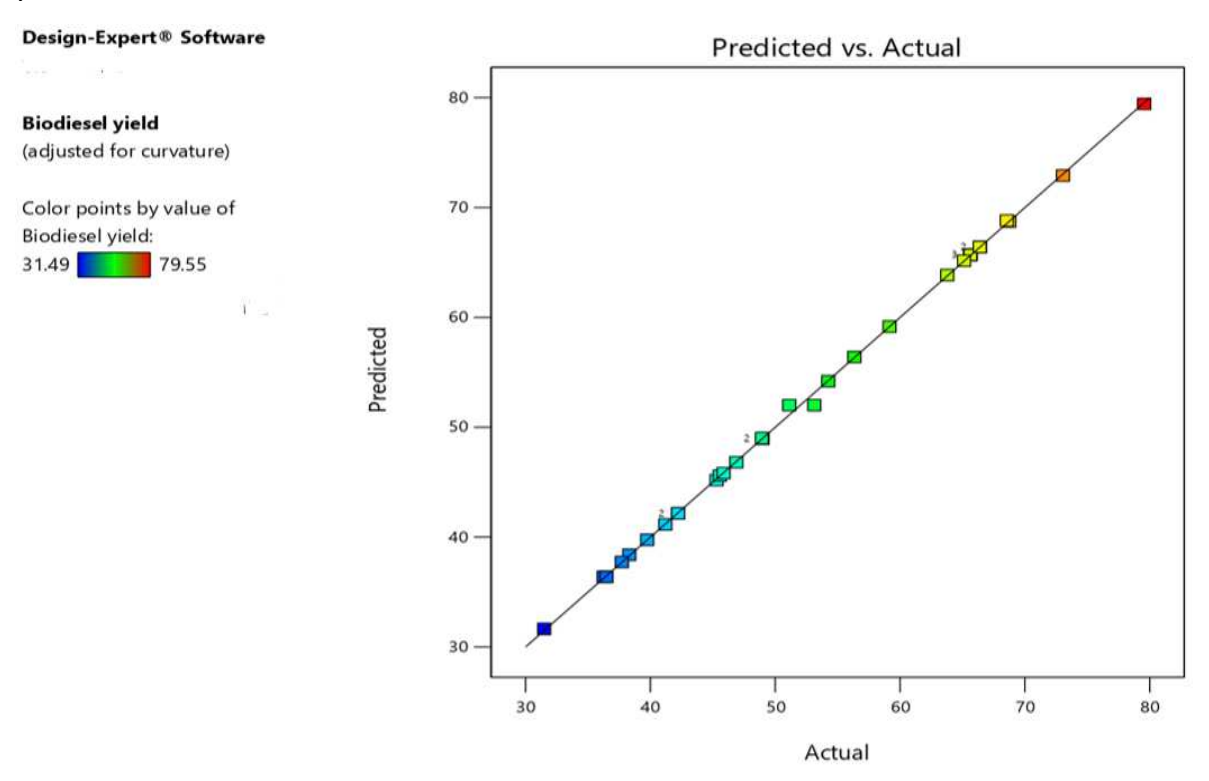
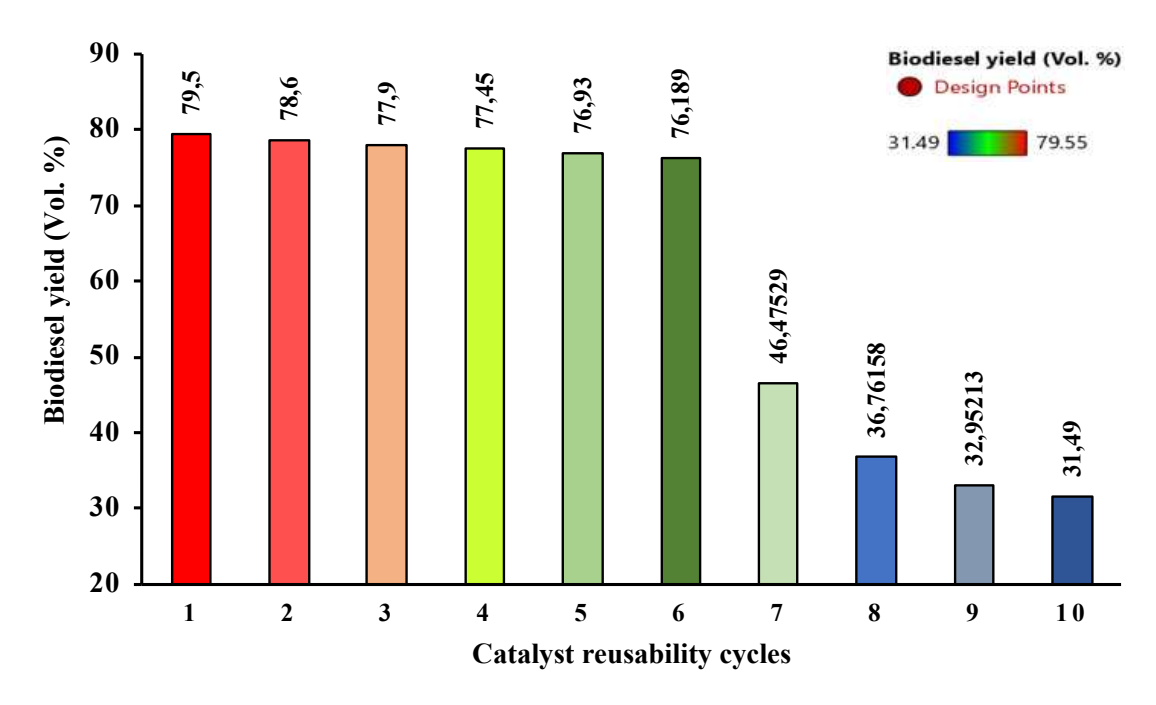


Figure 9. Predicted and actual yield for PKSOME.

# 3.4. Catalyst Regeneration

Catalyst reusability is a critical feature that influences the transesterification process, particularly in terms of cost. Catalyst dosage (A), methanol and oil mole ratio (B), temperature (C), reaction time (D), and agitation speed (E) were all taken into account. The reusability of the catalyst was investigated under optimal conditions by continuously recycling with optimal transesterification conditions (3 wt% of A, 8:1 of B, 55 °C of C, 90 min of D, and 250 rpm of E). The catalyst was washed with n-hexane and methanol after each experimental run under these conditions and then dried in an oven at 55 °C for 90 minutes. The recovered catalyst was used in the transesterification reaction for up to ten consecutive cycles. According to Figure 10, the catalyst did not experience a significant drop in catalyst activity and stability until the sixth cycle. The catalyst lost performance even more from the seventh to the tenth cycle, with a 61% drop when recovered after the sixth cycle. As a result, the catalyst can be recycled six times without experiencing leachability or a significant decrease in the catalytic performance or biodiesel yield.



**Figure 10**. Catalyst reusability for transesterification reaction.

# 3.5. Optimized Conditions for Synthesized PKSOME and Comparison with Heterogeneous Catalysts in Literature

Table 11 summarizes the optimal condition for the PKSOME. As detected, the maximum yield of PKSOME (79.55 %) was gotten with a catalyst dosage of 3.0 wt.%, methanol/oil molar ratio of 8.0/1, reaction temperature of 55 °C, reaction time of 90 minutes, and agitation speed of 250 rpm. The validation estimation exploiting the amended experimental constraints gave an experimental yield of 79.55%. The average error was detected as 0.011%. The validation outcomes established that the model was precise, as the extent of inaccuracy in the prediction was reliable. Table 12 compares the calcinated eggshell developed with those in the literature. As can be seen, the catalyst potency was greater than 75% in the sixth cycle run (See Figure 10). This validated the developed catalyst's reusability. The decrease in yield could be attributed to catalyst mesopores with fatty compositional deposition (Khan *et al.*, 2022).

#### 3.6. Commercial Viability of PKSOME Produced

To ensure the commercial viability of green diesel produced and to ensure satisfactory performance in IC engines, the fuels have to concur with the prerequisite established by ASTM D 6751 AND EN 14214 specifications (Samuel et al., 2019). **Table 13** compares the properties of PKSOME and other biodiesels. Basic fuel properties, such as kinematic viscosity, density, flash point, and acid values, were compared to those of biodiesels derived from palm oil (Roschat et al., 2016), and palm kernel oil (Alamu et al., 2008) as well as against various global standards, including ASTM D6751 (US) and EN 14214 (EU). The major properties compiled with the PKSOME produced confirm the green diesel's commercial viability in the market.

Reaction Reaction Catalyst Molar AS **Experiment** dosage temperature time P<sub>Y</sub> (%) E<sub>Y</sub> (%) **Error** ratio (rpm) (wt.%) (°C) (min.) 79.55 1 3.0 90 250 79.56 0.011 8:1 55

Table 11. Validation test.

**Table 12**. Comparison of developed eggshell catalyst heterogeneous catalyst with others in literature.

Catalyst type	Catalyst (wt.%)	Feedstock	Molar ratio	Reaction temperat ure (min)	Reacti on time (°C)	Speed (rpm)	*Y (%)/ru ns	Refs.
Calcinated eggshell catalyst	3.0	PKSO	8/1	55	90	250	79.6/ sixth cycle	Present study
Ca-Ce- Zn/Al2O3	8.19	Palm oil	18.53/ 1	180	66.12	NR	99.41	Qu <i>et al</i> . (2021)
Acid- treated golden apple snail shells	5	WCO	12/1	150	65	NR	97	Phewphon g et al. (2022)
Egg shell derived CaO	15	WCO	15/1	540	65	NR	95.45	Roschat <i>et al</i> . (2020)
NaOH	1.4	waste frying oil	6/1	180	58	305.5	91.6	Bello <i>et al</i> . (2016)
CaO/palmoi Imill fly ash	6	Crude palmoilCa	12/1	333 K	NS	700	75.73	Ho <i>et al</i> . (2014)
CaO/γ- Al2O3	6	Palm oil	12/1	338 K	NS	1000	98	Zabeti <i>et al</i> . (2009)

Table 13. Basic fuel properties of PKSOME.

Property	PKSOM E*	<b>Roschat et al.</b> (2016)	Alamu <i>et al</i> . (2008)	ASTM D6751	ASTM D6751	В0
Kinematic Viscosity @ 40 °C	3.2994	4.2	4.839	4.839	3.5-5.0	5.31
Refractive index @ 29 °C	1.4664	NS	ND	NS	NS	NS
Density @15 °C (g/cm <sup>3</sup> )	0.8927	0.875	0.883	Nil	0.85-0.90	0.85
Flash point	247	186	167	130 min	120 min	97
Cloud point	19.5	ND	6			NS
Acid value	0.504	0.24	ND	0.50 max	0.50 max	NS
Iodine value	18.3	NS	ND	NS	NS	ND
Oxidation Stability	3	15.44	ND	min 3	min 6	NS

#### 3.7. Cost of PKSOME

The cost of producing PKSOME is summarized in **Table 14**. As discovered, the estimated production costs of PKSOME (\$1.24 per liter) compared favorably with those in the literature (See **Table 14**). The cost differences can be attributed to the ethylic and methylic production of oily feedstocks, as well as the nature of the catalyst. If mass-produced, the cost of PKSOME could be competitive with that of fossil diesel. However, given the rising diesel price and the dependability of biodiesel feedstock sources, as well as the environmental benefits, applicability to the resident community, socioeconomic and topological stability, and energy security, the PKSOME pricing can be justified (Perumal & Ilangkumaran, 2018).

**Table 14**. Comparative of the cost of PKSOME with biodiesels, eco-friendly and consuming products.

Products	Generational feedstocks	Operative parameters on aggregate cost	Package	Manufacturing cost (USD)	Refs.
Brake pad	eggshells (Es) and banana peels (BPs)	Mass balance during the manufacturing process	Techno- economic analysis (TEA)	2.0/ piece Non- asbestos and asbestos-based brake pad	Nandiyanto et al. (2022)
Gold nanoparticles	Banana peel	Biosynthetic method	Economic evaluation	NS	Maratussolihah, et al., (2022)
MSW based biodiesel	<sup>a</sup> MSW	Petrieval ratio	Software	1.47/ liter	Gaeta-Bernardi and Parente (2016)
WCO biodiesel	WCO	Cleaned oil	Aspen	0.23-0.66/ liter	Khan <i>et al</i> . (2019)
Sludge derived biodiesel	Sludge	Extraction and transesterification from slush	Superpro Designer	0.67–1.07/ kg	Chen <i>et al</i> . (2018)
KO biodiesel	Karanja oil	Feedstocks expense, efficacy, and assorted charge	Economic simulation structure	1.23/ kg	Kumar <i>et al</i> . (2018)
CO biodiesel	Castor oil	Plant size and accessibility, oil content, labor responsibility, and harvesting	Aspen	0.28 /liter	Rahimi and Shafiei (2019)
Activated carbon and silica particles	Rice straw waste.	Fabrication	CAEE	NS	Nandiyanto (2018)
PKSOME	PKSO		Excel package	1.26 per liter	Present study
	Diesel	Nigeria		1.799 / liter	Price @ Dec. 2022

a: Municipal solid waste; CAEE: Cost analysis &economic evaluation; KO: Karanja oil; CO: Castor oil.

#### 3.8. Thermophysical Properties' Models for PKSOME

The correlation between density and viscosity, fire point and flash point, and aniline point and acid value vs. PKSOME content are shown in **Figure 11**. As shown in **Figure 11**, the density and viscosity values increased as the biodiesel content increased. The increase in density may compensate for PKSOME's lower energy content. Because of their high regression coefficients (R²) of 0.9924 and 0.9801, the parabolic equation  $(4x10^{-6}x^3 + 0.001x^2 + 0.0836x + 5.2593)$  and quadratic equation  $(-0.0011x^2 + 0.4575x + 848.13)$  are found suitable for the change of viscosity and density of PKSOME vs. biodiesel content. As depicted in **Figure 12**, the quadratic equations  $(0.0026x^2 + 0.1772x + 106.72)$  and  $(0.003x^2 + 0.1249x + 98.307)$  are used to fit the fire point (FIP) and flash point (FLP) at various PKSOME fractions. Increased FIP and FFP may lower fire risks and enhance PKSOME transport and storage (Di Serio *et al.*, 2008). The results are consistent with previous FLP findings (Al-Hamamre & Al-Salaymeh, 2014).

As illustrated in **Figure 13**, to fit the aniline point (AP) and acid value (AV) at various PKSOME fractions, the 2nd-degree equations  $(0.0005x^2-0.118x+52.079)$  and  $(0.000005x^2-0.0109x+0.9362)$  are used. Increased AP may improve PKSOME ignition properties and increase engine efficiency (Baghban & Adelizadeh, 2018). Higher AV, on the other hand, may not be advantageous because it can result in polymerization (Samuel & Gulum, 2019). Relationships between thermophysical properties (TPs) and PKSOME content as depicted in Figs. 11-13 (See **Table 15**). The varying content of PKSOME influences TPs, as shown by the curves.  $R^2$  values range from 0.993 to 0.999. Furthermore, refs. (Hoang, 2021; Samuel & Gulum, 2019; Wakil *et al.*, 2015) indicated that the TPs have a wide range of applications in the biodiesel industry.

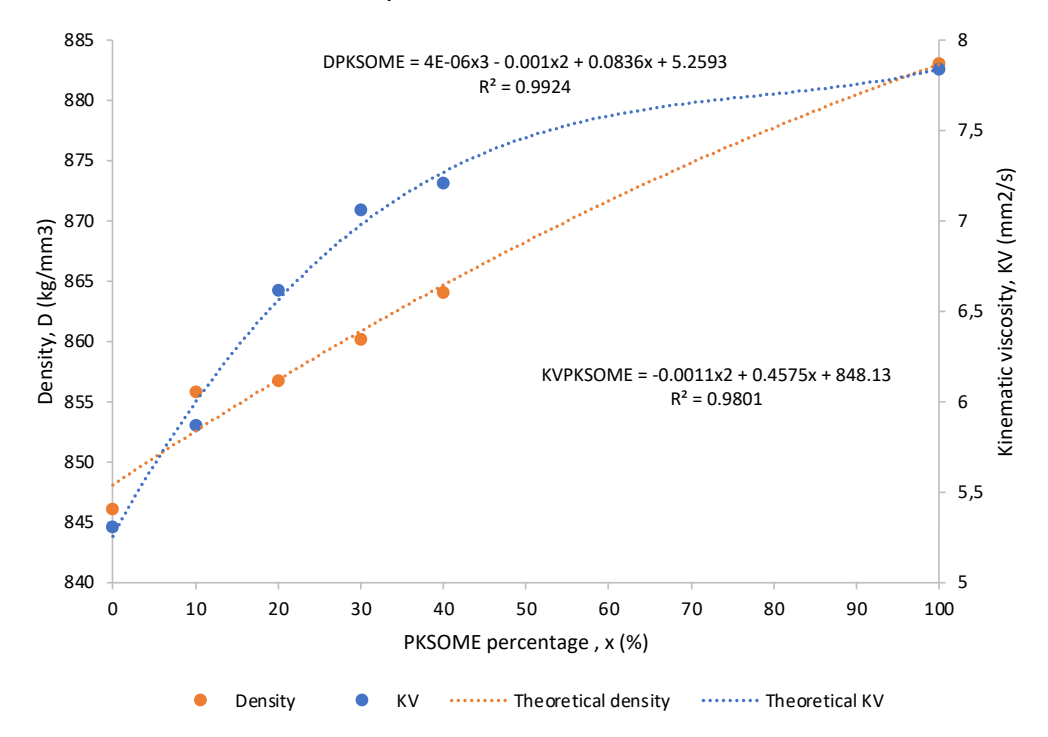


Figure 11. Variation of density and viscosity with PKSOME content.

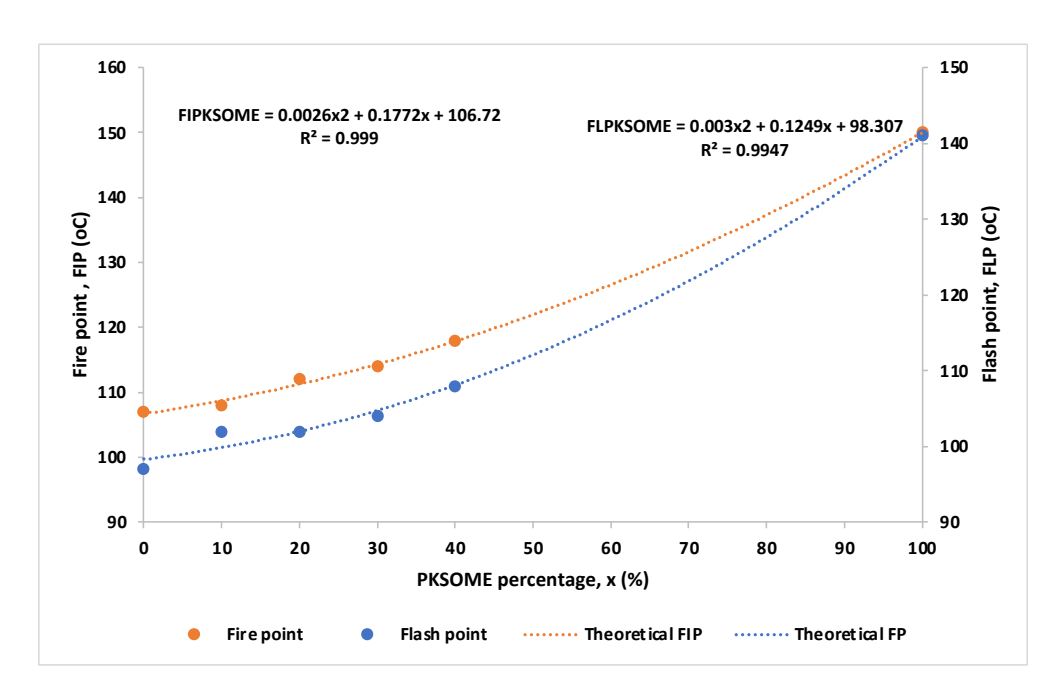


Figure 12. Variation of fire point and flash point with PKSOME content.

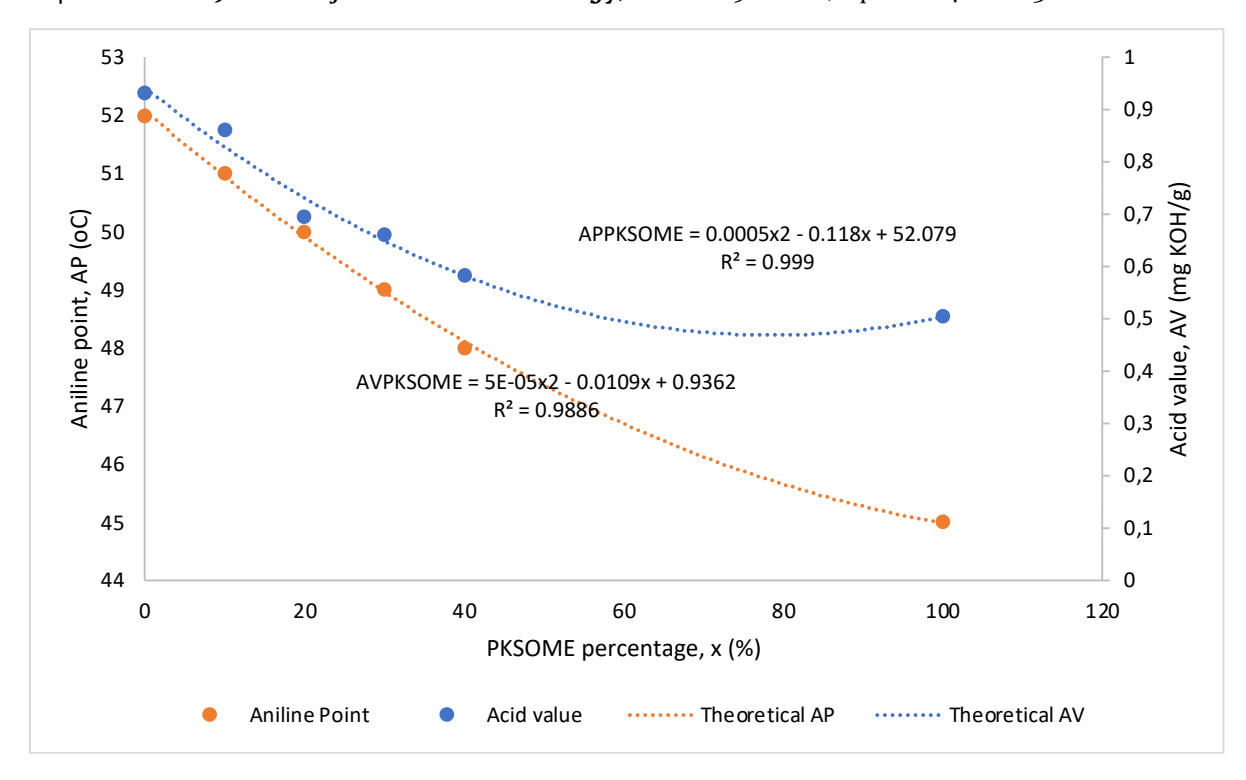


Figure 13. Variation of aniline point and acid value with PKSOME content.

**Table 15**. Correlation between TPs and PKSOME content (x).

Relations	Model equations	Possible applications	R <sup>2</sup>
D = f(x)	$D = 4x10^{-6}x^3 + 0.001x^2 + 0.0836x$	fuel supply system, fuel	0.993
	+ 5.2593	pump network (Hoang, 2021)	
V = f(x)	$V = 0.0011x^2 + 0.4575x$	fuel filters, spray	0.984
	+ 848.13	characteristics (Hoang, 2021)	
FFP = f(x)	$FFP = 0.0022x^2 + 0.1772x + 106.72$	Establishes the volatility of	0.999
		the green diesel	
FLP = f(x)	$FLP = 0.003x^2 + 0.1249x + 98.307$	Guarantee safety of	0.995
		transportable fuel and	
		measurement of	
		flammability of fuels (Wakil	
		et al., 2015)	
AP = f(x)	$AP = 0.0005x^2 - 0.118x + 52.079$	Checks the compatibility of	0.999
		green diesel with elastomers	
AV = f(x)	$AV = 0.000005x^2 - 0.0109x + 0.9362$	Tendency of fuel to	0.999
		polymerization (Samuel &	
		Gulum, 2019)	

# 3.9. Emission of Diesel PKSOME-fuelled Diesel Engine

# 3.9.1. Exhaust smoke emission

Figure 14 depicts the variation in smoke emission (SE) with different engine loads. As can be seen, the smoke increased as the load increased. Diesel fuel produced the most smoke when compared to the other fuels tested. This could be due to the higher oxygen content of the fuel compared to diesel fuel. In detail, the smoke emission at full load is 0.21 %vol. and 0.06%vol. for pure diesel and PKSOME, respectively. The SE for B 10, B20, B30, and B40 are 0.20, 0.17, 0.13, and 0.12 %vol, respectively. This also demonstrates complete biodiesel combustion in the fuel-rich area of the combustion chamber (Venu & Appavu, 2021).

### 3.9.2. Carbon (II) oxide

**Figure 15** depicts the variation of carbon monoxide emissions with engine load for PKSOME and diesel fuel blends. CO emission decreased as engine load increased at part load, as shown. This was caused by an increase in fuel consumption, which resulted in a rich air-fuel mixture. When compared to pure diesel fuel, biodiesel and its blends resulted in a substantial reduction in CO emission across the engine load range. This was due to biodiesel's higher oxygen content than diesel fuel, which resulted in more complete combustion (Kumar *et al.*, 2018).

# 3.9.3. Carbon (IV) oxide

**Figure 16** depicts the CO<sub>2</sub> emissions from the fuels under consideration. Carbon dioxide emissions from petro-diesel gradually increased with engine load, indicating more complete combustion at higher loads. Notably, the produced biodiesel exhibited nearly uniform combustion emission and exhaust data, indicating uniform combustion even at low loads. Such combustion uniformity is desirable and serves as a guideline for identifying a cleaner, environmentally friendly fuel.

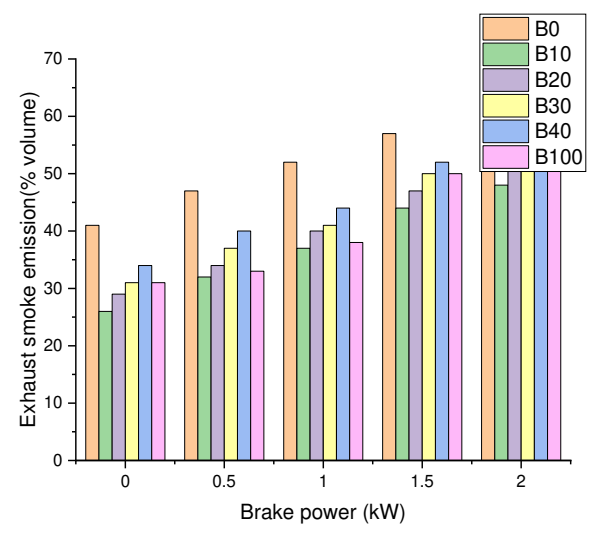


Figure 14. Smoke emission of different PKSOME and blends at different loads.

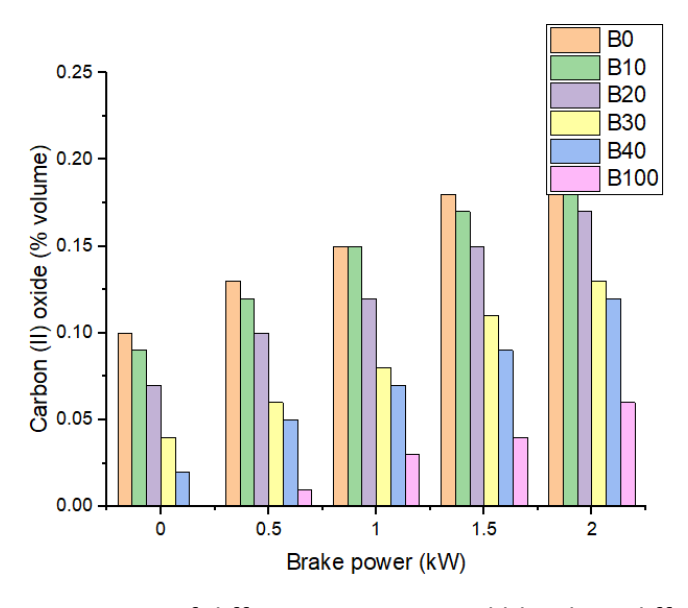


Figure 15. CO emission of different PKSOME and blends at different loads.

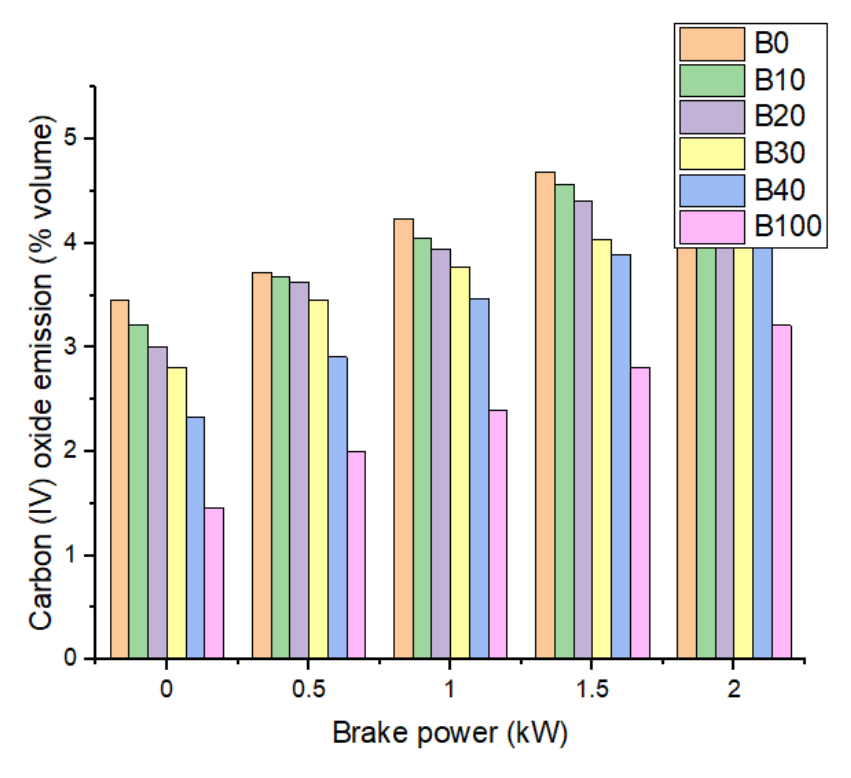


Figure 16. CO<sub>2</sub> emission of different PKSOME and blends at different loads.

#### 4. CONCLUSION

The study established the process optimization of heterogeneous catalyzed BPR from PKSO on the lab scale aided by the RSM. Correlation of TPs viz. density, viscosity, fire point and flash point, aniline point, and acid value of PKSOME produced and diesel blends were postulated. The cost of green diesel from PKSO and exhaustion emission study of assorted fuel types were investigated on IC engines. To obtain a notable study in the near future: (i) Exergetic, performance and emission features of nanoparticles and higher alcohol with PKSO biodiesel, (ii) spray and long performance of PKSO biodiesel as well as vibration features, (iii) Metaheuristics optimization algorithms of IC engines and boiler powered with aforementioned PKSO biodiesel and biogas, and bibliometric analysis of heterogeneous based biodiesel operated on IC engines be further studied. The following conclusions can be inferred from this study:

- (i) The optimum PKSOME yield (79.60%) was achieved with a catalyst dosage of 3.0 wt.%, molar ratio of 8/1, reaction temperature of 55 min, reaction time of 90 °C, and agitation speed of 250 rpm, as well as sixth cycle runs.
- (ii) The basic properties of PKSOME determined were following both ASTM D6751 and EN 14214 requirements.
- (iii) The commercial value of PKSOME was determined to be (1.26 USD/I) after cost estimation. The D was correlated with the PKSOME fraction using a parabolic equation, whereas the other TPs used 2nd-degree equations.
- (iv) Green diesel from PKSO and its diesel blends have lower tailpipe emissions than commercial diesel.
- (v) If mass-produced, the use of waste egg shell for heterogeneous catalyzed biodiesel from underutilized PKSO for green diesel can reduce production costs even further.
- (vi) The green biodiesel model and TP correlations have applications in the biodiesel and aviation industries.

#### 5. AUTHORS' NOTE

The authors declare that there is no conflict of interest regarding the publication of this article. The authors confirmed that the data and the paper are free of plagiarism. The authors made substantial contributions to the conception and design of the study. The authors took responsibility for data analysis, interpretation, and discussion of results. The authors read and approved the final manuscript.

#### 6. REFERENCES

- Abdul Aziz, S. M., Wahi, R., Ngaini, Z., Hamdan, S., and Yahaya, S. A. (2017). Esterification of microwave pyrolytic oil from palm oil kernel shell. *Journal of Chemistry*, *2017*, 1-9.
- Abdul Malek, A. B., Hasanuzzaman, M., and Rahim, N. A. (2020). Prospects, progress, challenges and policies for clean power generation from biomass resources. *Clean Technologies and Environmental Policy*, 22(6), 1229-1253.
- Adekoya, O., Oliyide, J., and Fasanya, I. (2022). Renewable and non-renewable energy consumption—Ecological footprint nexus in net-oil exporting and net-oil importing countries: Policy implications for a sustainable environment. *Renewable Energy, 189*, 524-534.
- Adepoju, T. F., Rasheed, B., Olatunji, O. M., Ibeh, M. A., Ademiluyi, F. T., and Olatunbosun, B. E. (2018). Modeling and optimization of lucky nut biodiesel production from lucky nut seed by pearl spar catalysed transesterification. *Heliyon*, 4(9), e00798.
- Ajala, E., Ehinmowo, A., Ajala, M., Ohiro, O., Aderibigbe, F., and Ajao, A. (2022). Optimisation of CaO-Al2O3-SiO2-CaSO4-based catalysts performance for methanolysis of waste lard for biodiesel production using response surface methodology and meta-heuristic algorithms. *Fuel Processing Technology*, 226, 107066.
- Alamu, O., Waheed, M., and Jekayinfa, S. (2008). Effect of ethanol—palm kernel oil ratio on alkali-catalyzed biodiesel yield. *Fuel*, *87*(8-9), 1529-1533.
- Al-Hamamre, Z., and Al-Salaymeh, A. (2014). Physical properties of (jojoba oil+biodiesel),(jojoba oil+diesel) and (biodiesel+diesel) blends. *Fuel*, 123, 175-188.
- Amesho, K., Lin, Y., Chen, C., Cheng, P., and Shangdiar, S. (2022). Kinetics studies of sustainable biodiesel synthesis from Jatropha curcas oil by exploiting bio-waste derived CaO-based heterogeneous catalyst via microwave heating system as a green chemistry technique. *Fuel, 323,* 123876.
- Ampah, J., Jin, C., Fattah, I., Appiah-Otoo, I., Afrane, S., Geng, Z., and Liu, H. (2022). Investigating the evolutionary trends and key enablers of hydrogen production technologies: A patent-life cycle and econometric analysis. *International Journal of Hydrogen Energy*, 2022, 1-22.
- Anjana, P., Niju, S., Begum, K., Anantharaman, N., Anand, R., and Babu, D. (2016). Studies on biodiesel production from Pongamia oil using heterogeneous catalyst and its effect on diesel engine performance and emission characteristics. *Biofuels*, 7(4), 377-387.

- Ashine, F., Kiflie, Z., Prabhu, S., Tizazu, B., Varadharajan, V., Rajasimman, M., Jayakumar, M. (2023). Biodiesel production from Argemone mexicana oil using chicken eggshell derived CaO catalyst. *Fuel*, *332*, 126166.
- Atelge, M. (2022). Production of biodiesel and hydrogen by using a double-function heterogeneous catalyst derived from spent coffee grounds and its thermodynamic analysis. *Renewable Energy*, 198, 1-15.
- Baghban, A., and Adelizadeh, M. (2018). On the determination of cetane number of hydrocarbons and oxygenates using adaptive neuro fuzzy inference system optimized with evolutionary algorithms. *Fuel*, *230*, 344-354.
- Balajii, M., and Niju, S. (2019). A novel biobased heterogeneous catalyst derived from Musa acuminata peduncle for biodiesel production—Process optimization using central composite design. *Energy Conversion and Management*, 189, 118-131.
- Bardhan, S., Gupta, S., Gorman, M., and Haider, M. (2015). Biorenewable chemicals: Feedstocks, technologies and the conflict with food production. *Renewable and Sustainable Energy Reviews*, 15, 506-520.
- Bazargan, A., Kostić, M., Stamenković, O., Veljković, V., and McKay, G. (2015). A calcium oxide-based catalyst derived from palm kernel shell gasification residues for biodiesel production. *Fuel*, *2015*, 519-525.
- Bello, E., Ogedengbe, T., Lajide, L., and Daniyan, I. (2016). Optimization of process parameters for biodiesel production using response surface methodology. *American Journal of Energy Engineering*, 4(2), 8-16.
- Betiku, E., and Ajala, S. (2014). Modeling and optimization of Thevetia peruviana (yellow oleander) oil biodiesel synthesis via Musa paradisiacal (plantain) peels as heterogeneous base catalyst: A case of artificial neural network vs. response surface methodology. *Industrial Crops and Products*, 53, 314-322.
- Bhikuning, A., and Senda, J. (2020). The properties of fuel and characterization of functional groups in biodiesel-water emulsions from waste cooking oil and its blends. *Indonesian Journal of Science and Technology*, *5*(1), 95-108.
- Chen, J., Tyagi, R. D., Li, J., Zhang, X., Drogui, P., and Sun, F. (2018). Economic assessment of biodiesel production from wastewater sludge. *Bioresource Technology*, 253, 41-48.
- Chimezie, E., Wang, Z., Yu, Y., Nonso, U., Duan, P., and Kapusta, K. (2023). Yield optimization and fuel properties evaluation of the biodiesel derived from avocado pear waste. *Industrial Crops and Products, 191*, 115884.
- Costa, E., Almeida, M., Alvim-Ferraz, M., and Dias, J. (2022). Exploiting the complementary potential of rice bran oil as a low-cost raw material for bioenergy production. *Processes*, 10(11), 2460.
- Dhawane, S., Kumar, T., and Halder, G. (2015). Central composite design approach towards optimization of flamboyant pods derived steam activated carbon for its use as heterogeneous catalyst in transesterification of Hevea brasiliensis oil. *Energy Conversion and Management*, 100, 277-287.

- Di Serio, M., Tesser, R., Pengmei, L., and Santacesaria, E. (2008). Heterogeneous catalysts for biodiesel production. *Energy and Fuels*, 22(1), 207-217.
- Dwivedi, G., Jain, S., Shukla, A., Verma, P., Verma, T., and Saini, G. (2022). Impact analysis of biodiesel production parameters for different catalyst. *Environment, Development and Sustainability*, 2022, 1-21.
- Elkelawy, M., Etaiw, S., Bastawissi, H., Marie, H., Radwan, A., Dawood, M., and Panchal, H. (2022). WCO biodiesel production by heterogeneous catalyst and using cadmium (II)-based supramolecular coordination polymer additives to improve diesel/biodiesel fueled engine performance and emissions. *Journal of Thermal Analysis and Calorimetry*, 147(11), 6375-6391.
- Farooq, M., Ramli, A., Naeem, A., Mahmood, T., Ahmad, S., Humayun, M., and Islam, M. G. (2018). Biodiesel production from date seed oil (Phoenix dactylifera L.) via egg shell derived heterogeneous catalyst. *Chemical Engineering Research and Design, 132*, 644-651.
- Fattah, I., Masjuki, H., Liaquat, A., Ramli, R., Kalam, M., and Riazuddin, V. (2013). Impact of various biodiesel fuels obtained from edible and non-edible oils on engine exhaust gas and noise emissions. *Renewable and Sustainable Energy Reviews*, 18, 552-567.
- Gaeta-Bernardi, A., and Parente, V. (2016). Organic municipal solid waste (MSW) as feedstock for biodiesel production: A financial feasibility analysis. *Renewable Energy, 86,* 1422-1432.
- Ghosh, N., and Halder, G. (2022). Current progress and perspective of heterogeneous nanocatalytic transesterification towards biodiesel production from edible and inedible feedstock: A review. *Energy Conversion and Management*, 270, 116292.
- Ginting, M., Azizan, M., and Yusup, S. (2012). Alkaline in situ ethanolysis of Jatropha curcas. *Fuel, 93*, 82-85.
- Gururani, P., Bhatnagar, P., Bisht, B., Jaiswal, K., Kumar, V., Kumar, S., and Rindin, K. (2022). Recent advances and viability in sustainable thermochemical conversion of sludge to bio-fuel production. *Fuel*, *316*, 123351.
- Haryanto, A., and Telaumbanua, M. (2020). Application of artificial neural network to predict biodiesel yield from waste frying oil transesterification. *Indonesian Journal of Science and Technology*, *5*(1), 62-74.
- Hidayat, A., Kurniawan, W., and Hinode, H. (2021). Sugarcane bagasse biochar as a solid catalyst: From literature review of heterogeneous catalysts for esterifications to the experiments for biodiesel synthesis from palm oil industry waste residue. *Indonesian Journal of Science and Technology*, 6(2), 337-352.
- Ho, W., Ng, H., Gan, S., and Tan, S. (2014). Evaluation of palm oil mill fly ash supported calcium oxide as a heterogeneous base catalyst in biodiesel synthesis from crude palm oil. *Energy Conversion and Management*, 88, 1167-1178.
- Hoang, A. (2021). Prediction of the density and viscosity of biodiesel and the influence of biodiesel properties on a diesel engine fuel supply system. *Journal of Marine Engineering and Technology*, 20(5), 299-311.

- Ishola, N., Okeleye, A., Osunleke, A., and Betiku, E. (2019). Process modeling and optimization of sorrel biodiesel synthesis using barium hydroxide as a base heterogeneous catalyst: appraisal of response surface methodology, neural network and neuro-fuzzy system. *Neural Computing and Applications*, 31(9), 4929-4943.
- Kareem, K., Rasheed, M., Liaquat, A., Hassan, A., Javed, M., and Asif, M. (2022). Clean energy production from jatropha plant as renewable energy source of biodiesel. *ASEAN Journal of Science and Engineering*, 2(2), 193-198.
- Kataria, J., Mohapatra, S., and Kundu, K. (2019). Biodiesel production from waste cooking oil using heterogeneous catalysts and its operational characteristics on variable compression ratio CI engine. *Journal of the Energy Institute*, *92*(2), 275-287.
- Khan, H., Ali, C., Iqbal, T., Yasin, S., Sulaiman, M., Mahmood, H., and Mu, B. (2019). Current scenario and potential of biodiesel production from waste cooking oil in Pakistan: An overview. *Chinese Journal of Chemical Engineering*, *27*(10), 2238-2250.
- Khan, I., Naeem, A., Farooq, M., Ghazi, Z., Saeed, T., Perveen, F., and Malik, T. (2022). Biodiesel production by valorizing waste non-edible wild olive oil using heterogeneous base catalyst: Process optimization and cost estimation. *Fuel, 320,* 123828.
- Kim, Y., Woo, D., and Kim, T. (2020). Characteristics of direct transesterification using ultrasound on oil extracted from spent coffee grounds. *Environmental Engineering Research*, 25(4), 470-478.
- Kirubakaran, M. (2018). Eggshell as heterogeneous catalyst for synthesis of biodiesel from high free fatty acid chicken fat and its working characteristics on a CI engine. *Journal of Environmental Chemical Engineering*, 6(4), 4490-4503.
- Kirubakaran, M. (2018). Eggshell as heterogeneous catalyst for synthesis of biodiesel from high free fatty acid chicken fat and its working characteristics on a CI engine. *Journal of Environmental Chemical Engineering*, 6(4), 4490-4503.
- Kolakoti, A., Kumar, A., Metta, R., Setiyo, M., and Rochman, M. (2022). Experimental studies on in-cylinder combustion, exergy performance, and exhaust emission in a Compression Ignition engine fuelled with neat biodiesels. *Indonesian Journal of Science and Technology*, 7(2), 219-236.
- Kumar, D., Singh, B., Banerjee, A., and Chatterjee, S. (2018). Cement wastes as transesterification catalysts for the production of biodiesel from Karanja oil. *Journal of Cleaner Production*, 183, 26-34.
- Kumar, H., Renita, A., and Jabasingh, S. (2021). Biodiesel production from preutilized cooking oil using a renewable heterogeneous eggshell-coconut pith catalyst: Process optimization and characterization. *Environmental Progress and Sustainable Energy*, 40(5), e13632.
- Kumar, M., Babu, A., and Kumar, P. (2018). The impacts on combustion, performance and emissions of biodiesel by using additives in direct injection diesel engine. *Alexandria Engineering Journal*, *57*(1), 509-516.
- Liu, K., Wang, R., and Yu, M. (2018). An efficient, recoverable solid base catalyst of magnetic bamboo charcoal: Preparation, characterization, and performance in biodiesel production. *Renewable Energy*, 127, 531-538.

- Maheshvari, R. (2022). Study on economic, sustainable development, and fuel consumption. *ASEAN Journal of Economic and Economic Education*, 1(1), 41-46.
- Maratussolihah, P., Rahmadianti, S., Tyas, K., Girsang, G., Nandiyanto, A., and Bilad, M. (2022). Techno-economic evaluation of gold nanoparticles using banana peel (Musa Paradisiaca). *ASEAN Journal for Science and Engineering in Materials.*, 1(1), 1-12.
- Mazaheri, H., Ong, H., Masjuki, H., Amini, Z., Harrison, M., Wang, C., and Alwi, A. (2018). Rice bran oil based biodiesel production using calcium oxide catalyst derived from Chicoreus brunneus shell. *Energy*, *144*, 10-19.
- Mendonça, I., Paes, O., Maia, P., Souza, M., Almeida, R., Silva, C., and de Freitas, F. (2019). New heterogeneous catalyst for biodiesel production from waste tucumã peels (Astrocaryum aculeatum Meyer): Parameters optimization study. *Renewable Energy*, 130, 103-110.
- Moser, B. (2009). Biodiesel production, properties, and feedstocks. *Vitro Cell Dev Biol-Plant,* 45, 229–66.
- Nair, J., SatyanarayanaMurthy, Y., and Javed, S. (2020). Combustion and emission characteristics of light duty diesel engine fueled with transesterified algae biodiesel by K2CO3/ZnO heterogeneous base catalyst. *Energy Sources, Part A: Recovery, Utilization, and Environmental Effects*, 42, 1-13.
- Nandiyanto, A. (2018). Cost analysis and economic evaluation for the fabrication of activated carbon and silica particles from rice straw waste. *Journal of Engineering, Science and Technology*, 13(6), 1523-1539.
- Nandiyanto, A. B. D., Ragadhita, R., and Fiandini, M. (2023). Interpretation of Fourier transform infrared spectra (FTIR): A practical approach in the polymer/plastic thermal decomposition. *Indonesian Journal of Science and Technology*, 8(1), 113-126.
- Nandiyanto, A., Oktiani, R., and Ragadhita, R. (2019). How to read and interpret FTIR spectroscope of organic material. *Indonesian Journal of Science and Technology, 4*(1), 97-118.
- Nandiyanto, A., Ragadhita, R., Fiandini, M., Al Husaeni, D., Al Husaeni, D., and Fadhillah, F. (2022). Domestic waste (eggshells and banana peels particles) as sustainable and renewable resources for improving resin-based brakepad performance: Bibliometric literature review, techno-economic analysis, dual-sized reinforcing experiments, to comparison with c. *Communications in Science and Technology*, 7(1), 50-61.
- Narula, V., Khan, M., Negi, A., Kalra, S., Thakur, A., and Jain, S. (2017). Low temperature optimization of biodiesel production from algal oil using CaO and CaO/Al2O3 as catalyst by the application of response surface methodology. *Energy*, *140*, 879-884.
- Nayaggy, M., and Putra, Z. (2019). Process simulation on fast pyrolysis of palm kernel shell for production of fuel. *Indonesian Journal of Science and Technology*, 4(1), 64-73.
- Nema, V. K., Singh, A., Chaurasiya, P. K., Gogoi, T. K., Verma, T. N., and Tiwari, D. (2023). Combustion, performance, and emission behavior of a CI engine fueled with different biodiesels: A modelling, forecasting and experimental study. *Fuel*, *339*, 126976.

- Obinna, E. (2022). Physicochemical properties of human hair using Fourier transform infrared (FTIR) and scanning electron microscope (SEM). *ASEAN Journal for Science and Engineering in Materials*, 1(2), 71-74.
- Ofori-Boateng, C., and Lee, K. (2013). The potential of using cocoa pod husks as green solid base catalysts for the transesterification of soybean oil into biodiesel: Effects of biodiesel on engine performance. *Chemical Engineering Journal*, 220, 395-401.
- Ong, H., Masjuki, H., Mahlia, T., Silitonga, A., Chong, W., and Leong, K. (2014). Optimization of biodiesel production and engine performance from high free fatty acid Calophyllum inophyllum oil in CI diesel engine. *Energy conversion and Management*, 81, 30-34.
- Osman, A., Mehta, N., Elgarahy, A., Al-Hinai, A., Al-Muhtaseb, A., and Rooney, D. (2021). Conversion of biomass to biofuels and life cycle assessment: A review. *Environmental Chemistry Letters*, 19(6), 4075-4118.
- Oti, O., Nwaigwe, K., and Okereke, N. (2017). Assessment of palm kernel shell as a composite aggregate in concrete. *Agricultural Engineering International: CIGR Journal*, 19(2), 34-41.
- Patel, R., and Sankhavara, C. (2020). Investigation of performance and emissions of diesel engine run on biodiesel produced from karanja oil in a single-step transesterification process using heterogeneous catalyst (lithium-impregnated calcium oxide). *Biofuels*, 11(4), 421-430.
- Pebrianti, M., and Salamah, F. (2021). Learning simple pyrolysis tools for turning plastic waste into fuel. *Indonesian Journal of Multidiciplinary Research*, 1(1), 99-102.
- Perumal, V., and Ilangkumaran, M. (2018). Experimental analysis of operating characteristics of a direct injection diesel engine fuelled with Cleome viscosa biodiesel. *Fuel*, 224, 379-387.
- Phewphong, S., Roschat, W., Pholsupho, P., Moonsin, P., Promarak, V., and Yoosuk, B. (2022). Biodiesel production process catalyzed by acid-treated golden apple snail shells (Pomacea canaliculata)-derived CaO as a high-performance and green catalyst. *Engineering and Applied Science Research, 49*(1), 36-46.
- Pradhan, P., and Chakraborty, R. (2018). Optimal efficient biodiesel synthesis from used oil employing low-cost ram bone supported Cr catalyst: Engine performance and exhaust assessment. *Energy, 164,* 35-45.
- Pradhan, P., Chakraborty, S., and Chakraborty, R. (2016). Optimization of infrared radiated fast and energy-efficient biodiesel production from waste mustard oil catalyzed by Amberlyst 15: Engine performance and emission quality assessments. *Fuel*, *173*, 60-68.
- Qu, T., Niu, S., Zhang, X., Han, K., and Lu, C. (2021). Preparation of calcium modified Zn-Ce/Al2O3 heterogeneous catalyst for biodiesel production through transesterification of palm oil with methanol optimized by response surface methodology. *Fuel, 284*, 118986.
- Rahimi, V., and Shafiei, M. (2019). Techno-economic assessment of a biorefinery based on low-impact energy crops: A step towards commercial production of biodiesel, biogas, and heat. *Energy Conversion and Management, 183,* 698-707.

- Razzaq, L., Imran, S., Anwar, Z., Farooq, M., Abbas, M., Mehmood Khan, H., and Rizwanul Fattah, I. (2020). Maximising yield and engine efficiency using optimised waste cooking oil biodiesel. *Energies*, *13*(22), 5941.
- Rezania, S., Korrani, Z., Gabris, M., Cho, J., Yadav, K., Cabral-Pinto, M., and Nodeh, H. (2021). Lanthanum phosphate foam as novel heterogeneous nanocatalyst for biodiesel production from waste cooking oil. *Fuel*, *176*, 228-236.
- Rodrigues, S., Mazzone, L., Santos, F., Cruz, M., and Fernandes, F. (2009). Optimization of the production of ethyl esters by ultrasound assisted reaction of soybean oil and ethanol. *Brazilian Journal of Chemical Engineering*, *26*, 361-366.
- Roschat, W., Butthichak, P., Daengdet, N., Phewphong, S., Kaewpuang, T., Moonsin, P., and Promarak, V. (2020). Kinetics study of biodiesel production at room temperature based on eggshell-derived CaO as basic heterogeneous catalyst. *Engineering and Applied Science Research*, 47(4), 361-373.
- Roschat, W., Siritanon, T., Yoosuk, B., and Promarak, V. (2016). Biodiesel production from palm oil using hydrated lime-derived CaO as a low-cost basic heterogeneous catalyst. *Energy Conversion and Management, 108,* 459-467.
- Rupani, P., Zabed, H., and Domínguez, J. (2022). Vermicomposting and bioconversion approaches towards the sustainable utilization of palm oil mill waste. *Advanced Organic Waste Management*, 2022, 193-205.
- Samuel, O. D., and Emovon, I. (2018). The development of expeller for kernel based seed and its oil characterization. *International Journal of Integrated Engineering*, 10(1), 176-181.
- Samuel, O., and Gulum, M. (2019). Mechanical and corrosion properties of brass exposed to waste sunflower oil biodiesel-diesel fuel blends. *Chemical Engineering Communications*, 206(5), 682-694.
- Samuel, O., Kaveh, M., Oyejide, O., Elumalai, P., Verma, T., Nisar, K., and Sarıkoç, S. (2022b). Performance comparison of empirical model and Particle Swarm Optimization and its boiling point prediction models for waste sunflower oil biodiesel. *Case Studies in Thermal Engineering*, 33, 101947.
- Samuel, O., Kaveh, M., Verma, T., Okewale, A., Oyedepo, S., Abam, F., and Szymane, M. (2022a). Grey wolf optimizer for enhancing nicotiana tabacum I. oil methyl ester and prediction model for calorific values. *Case Studies in Thermal Engineering*, *35*, 102095.
- Samuel, O., Okwu, M., Amosun, S., Verma, T., and Afolalu, S. (2019). Production of fatty acid ethyl esters from rubber seed oil in hydrodynamic cavitation reactor: Study of reaction parameters and some fuel properties. *Industrial Crops and Products, 141*, 111658.
- Sarve, A., Sonawane, S., and Varma, M. (2015). Ultrasound assisted biodiesel production from sesame (Sesamum indicum L.) oil using barium hydroxide as a heterogeneous catalyst: Comparative assessment of prediction abilities between response surface methodology (RSM) and artificial neural network (ANN). *Ultrasonics Sonochemistry*, 26, 218-228.
- Setiyo, M., Yuvenda, D., and Samuel, O. (2021). The latest report on the advantages and disadvantages of pure biodiesel (B100) on engine performance: Literature review and bibliometric analysis. *Indonesian Journal of Science and Technology*, 6(3), 469-490.

- Singh, A., Sinha, S., Choudhary, A., Panchal, H., Elkelawy, M., and Sadasivuni, K. (2020). Optimization of performance and emission characteristics of CI engine fueled with Jatropha biodiesel produced using a heterogeneous catalyst (CaO). *Fuel*, 280, 118611.
- Singh, V., Belova, L., Singh, B., and Sharma, Y. (2018). Biodiesel production using a novel heterogeneous catalyst, magnesium zirconate (Mg2Zr5O12): Process optimization through response surface methodology (RSM). *Energy Conversion and Management,* 174, 198-207.
- Singh, Y., Sharma, A., Tiwari, S., and Singla, A. (2019). Optimization of diesel engine performance and emission parameters employing cassia tora methyl esters-response surface methodology approach. *Energy*, *168*, 909-918.
- Sukamto, S., and Rahmat, A. (2023). Evaluation of FTIR, macro and micronutrients of compost from black soldier fly residual: In context of its use as fertilizer. *ASEAN Journal of Science and Engineering*, 3(1), 21-30.
- Sundaramahalingam, M., Karthikumar, S., Kumar, R., Samuel, K., Shajahan, S., Sivasubramanian, V., and Elgorban, A. (2021). An intensified approach for transesterification of biodiesel from Annona squamosa seed oil using ultrasound-assisted homogeneous catalysis reaction and its process optimization. *Fuel, 291*, 120195.
- Tamilarasan, S., and Sahadevan, R. (2014). Ultrasonic assisted acid base transesterification of algal oil from marine macroalgae Caulerpa peltata: Optimization and characterization studies. *Fuel*, *128*, 347-355.
- Tang, Z., Lim, S., Pang, Y., Ong, H., and Lee, K. (2018). Synthesis of biomass as heterogeneous catalyst for application in biodiesel production: State of the art and fundamental review. *Renewable and Sustainable Energy Reviews*, *92*, 235-253.
- Thushari, I., Babel, S., and Samart, C. (2019). Biodiesel production in an autoclave reactor using waste palm oil and coconut coir husk derived catalyst. *Renewable Energy, 134*, 125-134.
- Venu, H., and Appavu, P. (2021). Combustion and emission characteristics of tamarind seed biodiesel-diesel blends in a compression ignition engine. *International Journal of Ambient Energy*, 42(12), 1441-1446.
- Veza, I., Zainuddin, Z., Tamaldin, N., Idris, M., Irianto, I., and Fattah, I. (2022). Effect of palm oil biodiesel blends (B10 and B20) on physical and mechanical properties of nitrile rubber elastomer. *Results in Engineering*, *16*, 100787.
- Wakil, M., Kalam, M., Masjuki, H., Atabani, A., and Fattah, I. (2015). Influence of biodiesel blending on physicochemical properties and importance of mathematical model for predicting the properties of biodiesel blend. *Energy Conversion and Management, 94*, 51-67.
- Wongjaikham, W., Kongprawes, G., Wongsawaeng, D., Ngaosuwan, K., Kiatkittipong, W., Hosemann, P., and Assabumrungrat, S. (2021). Highly effective microwave plasma application for catalyst-free and low temperature hydrogenation of biodiesel. *Fuel, 305*, 121524.

- Yaşar, F. (2019). Biodiesel production via waste eggshell as a low-cost heterogeneous catalyst: Its effects on some critical fuel properties and comparison with CaO. *Fuel, 255*, 115828.
- Yolanda, Y. D., and Nandiyanto, A. B. (2022). How to read and calculate diameter size from electron microscopy images. *ASEAN Journal of Science and Engineering Education*, 2(1), 11-36.
- Zabeti, M., Daud, W., and Aroua, M. (2009). Optimization of the activity of CaO/Al2O3 catalyst for biodiesel production using response surface methodology. *Applied Catalysis A: General,* 366(1), 154-159.
- Zhao, C., Lv, P., Yang, L., Xing, S., Luo, W., and Wang, Z. (2018). Biodiesel synthesis over biochar-based catalyst from biomass waste pomelo peel. *Energy Conversion and Management*, 160, 477-485.